

255435 ✓

DP - 515

REACTORS - POWER  
(TID-4500, 15th Ed.)

**HEAVY WATER MODERATED POWER REACTORS**  
**Progress Report**  
**June 1960**

D. F. Babcock, Coordinator  
Power Reactor Studies  
Wilmington, Delaware

Compiled by R. R. Hood and L. Isakoff

August 1960

*Issued October 1960*

E. I. du Pont de Nemours & Co.  
Explosives Department - Atomic Energy Division  
Technical Division - Wilmington, Delaware

Printed by Savannah River Laboratory for  
The United States Atomic Energy Commission  
Contract AT(07-2)-1

RECORDS ADMINISTRATION



R1046742

### ABSTRACT

At the end of June 1960, 36% of the construction and 94% of the firm design of the Heavy Water Components Test Reactor (HWCTR) were complete. Revised calculations of transients in the liquid-D<sub>2</sub>O-cooled loop of the HWCTR show that the safety of the loop is not impaired by recent changes in the location and design of the loop heat exchanger. Preliminary operation of a full-scale mockup of the bayonet for the boiling-D<sub>2</sub>O-cooled loop of the HWCTR indicates that flow-induced vibrations probably will not be a serious problem in this loop. Irradiation specimens were prepared of Zircaloy-clad tubes of uranium oxide that had been vibratory-compacted and swaged to 91% of theoretical density. The NRU irradiation of a Zircaloy-clad uranium metal fuel tube was terminated because of mechanical damage to the assembly during an attempted reinsertion into the reactor loop. Tandem-extruded joints of Zircaloy to stainless steel were readied for long-term irradiation tests to determine the effects of exposure on the mechanical properties of the joints.

## CONTENTS

	<u>Page</u>
List of Tables and Figures	4
Introduction	6
Summary	6
Discussion	8
I. Heavy Water Components Test Reactor (HWCTR)	8
A. Status of Design and Construction	8
B. Safeguards Analyses of Liquid D <sub>2</sub> O Loop	8
1. Steady-State Conditions	9
2. Transients Following a Scram	9
3. Transients Following Increases in Reactivity	9
4. Transients Following Loss of H <sub>2</sub> O Flow	10
5. Transients Following an AC Power Failure	10
6. Transients Following Changes in Heat Exchanger Bypass Flow	11
C. Mockup of Bayonet for Boiling Loop	11
D. Leak Testing of Bayonet Joints	13
E. Mechanical Joints for Fuel Housings	14
II. Technology of Full-Scale Reactors	14
A. Physics Studies	14
1. Boiling-D <sub>2</sub> O-Cooled Power Reactors	14
a. Void Coefficients	14
b. Power Coefficient of Boiling D <sub>2</sub> O Reactors Fueled with Oxide Tubes	15
2. Neutron Slowing-Down Distribution	16
3. The (n,2n) Reaction with Deuterium	18
B. Reactor Fuels and Materials	19
1. Fuel Elements of Uranium Metal	19
a. Thin-Walled Coextruded Tubes	19
2. Fuel Elements of Uranium Oxide	20
a. Swaged Tubes Clad with Zircaloy	20
b. Uranium Metal Impurity in Fused Uranium Oxide	21
3. Cladding Studies	21
a. Development of Zirconium Cladding Alloys	21
b. Swaged Cladding	21

	<u>Page</u>
4. Zircaloy-to-Stainless-Steel Joints	22
C. Irradiation Testing	23
1. Tubes of Uranium Metal	23
a. Unalloyed Uranium Tube in the NRU Reactor	23
b. Lead-Insulated Uranium Tubes	23
2. Tandem-Extruded Joints of Zircaloy to Stainless Steel	24
D. Engineering Studies	24
1. Design of Fuel Assemblies Cooled by Boiling D <sub>2</sub> O	24
2. Mechanical Seals for Pumps	24
Bibliography	26

#### LIST OF TABLES AND FIGURES

##### Table

I	Proposed Test Conditions for Bayonet Mockup	28
II	Exit Steam Qualities for Fuel Rod Clusters Cooled by Boiling Water	28
III	Leakage Data from Bench Tests of "Durametallc" Mechanical Seals	29

##### Figure

1	Steady-State D <sub>2</sub> O Temperatures in Liquid D <sub>2</sub> O Loop of HWCTR	30
2	Transients in Liquid D <sub>2</sub> O Loop of HWCTR After Reactor Scram	31
3	Transients in Liquid D <sub>2</sub> O Loop of HWCTR After Sudden Loss of H <sub>2</sub> O Flow to Loop Heat Exchanger	32
4	Transients in Liquid D <sub>2</sub> O Loop of HWCTR After AC Power Failure	33
5	Transients in Liquid D <sub>2</sub> O Loop of HWCTR After Decrease in Bypass Flow Around Loop Heat Exchanger	34
6	Transients in Liquid D <sub>2</sub> O Loop of HWCTR After Increase in Bypass Flow Around Loop Heat Exchanger	35
7	Mockup of Bayonet for HWCTR Boiling D <sub>2</sub> O Loop	36
8	Flow Diagram of HWCTR Bayonet Test Loop	37
9	Fuel Rod Bundle for Mockup of HWCTR Bayonet	38
10	Enclosure and Mounting Details for Mockup of HWCTR Boiling Bayonet	39

<u>Figure</u>		<u>Page</u>
11	Test Arrangement of "Conoseal" Joint for Coolant Connections of HWCTR Bayonet	40
12	Test Arrangement of "Grayloc" Joint for Coolant Connections of HWCTR Bayonet	41
13	Test Arrangement of Top Closure for HWCTR Bayonet	42
14	Zircaloy Housing Flared Joint	43
15	Effective Void Fraction in a Boiling D <sub>2</sub> O Reactor	44
16	Effect of a 1% Increase in Power on the Void Fraction in a Boiling D <sub>2</sub> O Reactor	44
17	Power Coefficients of Reactivity for Boiling-D <sub>2</sub> O-Cooled Power Reactors Fueled with UO <sub>2</sub> Tubes	45
18	Indium Foil Activity Distributions From Various Sources	46
19	Foil Activity Distributions with a Single Enriched Uranium Rod as a Source	47
20	Self-Resonance Capture Ratio for Isolated Fuel Elements in D <sub>2</sub> O	48
21	Uranium Metal Impurity in Fused UO <sub>2</sub>	49
22	Lead-Insulated Tubular Uranium Specimen	50
23	Irradiation Specimen of a Tandem-Extruded Joint of Zircaloy to Stainless Steel	51
24	"Durametalllic" Mechanical Seal for Bench Testing	52
25	Bench Tester for Mechanical Seals	53

# HEAVY WATER MODERATED POWER REACTORS

Progress Report  
June 1960

## INTRODUCTION

This report is one of a series that records the progress of the du Pont study of power reactors that are moderated by heavy water and fueled with natural uranium. The present effort is divided into two main categories: (1) the development required for the successful design, construction, and operation of the Heavy Water Components Test Reactor (HWCTR), a facility for irradiating fuel elements and testing other components at power reactor conditions, and (2) the development of the technology of full-scale D<sub>2</sub>O-moderated power reactors. Earlier reports in the series are:

DP-232	DP-375	DP-445
DP-245	DP-385	DP-455
DP-265	DP-395	DP-465
DP-285	DP-405	DP-475
DP-295	DP-415	DP-485
DP-315	DP-425	DP-495
DP-345	DP-435	DP-505

Progress during July 1960 will be reported in DP-525.

## SUMMARY

At the end of June, 36% of the construction and 94% of the design of the HWCTR were complete. Approximately 70% of the design work for the isolated coolant loops was also completed by the end of this report period.

Revised calculations of transients in the liquid D<sub>2</sub>O loop of the HWCTR show that the safety of the loop is not impaired by changing the D<sub>2</sub>O flow path in the heat exchanger and by relocating the surge tank downstream of the heat exchanger. These design changes make the loop more sluggish in its response to disturbances, and the transients are generally milder than those computed for the original loop design.

Preliminary operation of a full-scale mockup of the bayonet for the boiling loop of the HWCTR indicates that vibration probably will not be a serious problem in the HWCTR bayonet. No vibration of the mockup was detected visually when 4,100 lb/hr of superheated steam at 430°C and 850 psia was dispersed into 22,000 lb/hr of water flowing into the bayonet at 220°C. The exit steam quality was 14%.

The average leakage of water from a candidate joint for coolant connections of the HWCTR bayonets was within design limits of 40 lb/yr throughout 89 thermal cycles at peak conditions of 250°C and 850 psig. In the next 10 cycles, the leakage increased markedly and far exceeded the design limit.

Ten 4-foot-long tubes of Zircaloy-clad uranium oxide were fabricated at Savannah River Laboratory by vibratory compaction and swaging. The oxide was initially vibrated to 72% of theoretical density and then cold swaged to final dimensions and a density of 91% of theoretical. Eighteen 2-foot-long specimens were prepared from these tubes; six are for irradiation in a Savannah River reactor and the remainder are for out-of-pile evaluation tests.

The irradiation test of a Zircaloy-clad uranium metal tube under power reactor conditions in a liquid-cooled loop of the NRU reactor was terminated because of mechanical difficulties. A maximum exposure of 950 MWD/T had been reached with an accompanying maximum volume increase of 1.5% and a maximum outer cladding strain of 0.14%. It was intended that the test be continued but after repeated attempts to reload the tube into the loop, severe damage to the shroud, scratching of the clad surface, and excessive bowing of the tube were observed. Additional irradiation was no longer feasible. No further testing of metal fuel is currently scheduled for the Chalk River loop.

Preparations were made for the irradiation of tandem-extruded joints under a tensile load to determine the effects of long periods of fast neutron exposure on the mechanical properties of the joint. The test specimens are designed for irradiation at relatively low temperature in the central core of a Savannah River reactor. In this position, the joints will accumulate exposure at a much more rapid rate than they would in power reactor application where the joints would be located somewhat removed from the edge of the core. Thus, the equivalent of a lifetime of power reactor exposure can be obtained in less than one year of test.

## DISCUSSION

### I. HEAVY WATER COMPONENTS TEST REACTOR (HWCTR)

The HWCTR is a test reactor that is being built at the Savannah River Plant for the purpose of irradiating candidate fuel assemblies and other reactor components under conditions that are representative of D<sub>2</sub>O-moderated power reactors. It is scheduled to be placed in operation in mid-1961. A description of the facility was presented in DP-383<sup>(1)</sup> and in earlier progress reports. Progress during June on design, construction, and supporting studies is reported in this section.

#### A. STATUS OF DESIGN AND CONSTRUCTION

The principal construction activity during June was the erection of the steel superstructure of the reactor containment vessel by the Chicago Bridge and Iron Co. At the end of the month, the erection was about 20% complete. Design activity is largely complete except for necessary field design changes. About 75% of the scheduled drawings have been issued for the two isolated coolant loops, and procurement of all major equipment for the loops has been started.

The over-all design and construction status at the end of June was:

Design of reactor system and building	- 94% complete
Design of isolated loops	- 70% complete
Reactor construction	- 36% complete

#### B. SAFEGUARDS ANALYSES OF LIQUID D<sub>2</sub>O LOOP

Calculations of the transient response of the liquid-D<sub>2</sub>O-cooled loop to various disturbances were reported in DP-445 and DP-465. Subsequently, several changes were made in the design of the loop, the principal ones being (1) relocation of the surge tank to a position downstream of the heat exchanger, and (2) passage of the D<sub>2</sub>O flow through the shell side of the heat exchanger rather than through the tubes. The results of revised calculations of loop kinetics show that the safety of the loop is not impaired by these design changes and that no new safety problems arise from the changes. In general, the redesigned loop is more sluggish in its response to disturbances, because of the increased volume of cool D<sub>2</sub>O in the heat exchanger and surge tank, and the transients are milder than those computed for the original design.

The results of the revised calculations are presented in the following paragraphs. The equations that were used in the calculations are similar to those that were derived for analyzing the transients in the primary coolant system of the HWCTR (DP-245, pp. 33-37). A description of the loop was presented in DP-415. In normal HWCTR operation, the loop pressure will be higher than the reactor pressure by as much as 500 psi. Rupture discs between the gas pressurizing systems of the loop and the

reactor are designed to rupture when the loop pressure is either 700 psi higher than reactor pressure or 200 psi lower than reactor pressure.

### 1. Steady-State Conditions

Figure 1 shows the new steady-state temperatures in the loop for a constant reactor power of 50 MW and as a function of the fraction,  $f$ , of the loop  $D_2O$  that is bypassed around the heat exchanger. If more than 92.6% of the design flow (260 gpm) were bypassed, the  $D_2O$  at the outlet of the fuel assembly in the loop would boil. A value of  $f = 0.90$  was adopted for the kinetics calculations. This choice yields initial  $D_2O$  temperatures of  $252^\circ C$  at the inlet to the fuel assembly and  $273^\circ C$  at the outlet of the assembly. The corresponding design values for the loop are 250 and  $274^\circ C$ , respectively.

### 2. Transients Following a Scram

Figure 2 shows temperature and pressure transients in the loop following a reactor scram from a power level of 50 MW. The loop pressure and the difference between loop pressure and reactor pressure were computed on the basis of an initial gas volume of 55 gallons in the loop surge tank. It was also assumed that the steam valves on the reactor boilers are left open at their 50 MW steady-state settings, and that a constant 90% of the loop  $D_2O$  flow is bypassed around the loop heat exchanger. It is seen from Figure 2 that under these conditions the pressure differential between the loop and the reactor is not large enough to rupture the discs between the two systems.

### 3. Transients Following Increases in Reactivity

If a half rod falls from the center of the HWCTR core to the bottom as a result of a broken latch, the reactivity may be suddenly increased by as much as 0.006 k. It is shown in DP-383<sup>(1)</sup> that if the reactivity increase were this great, the safety rods would not act fast enough to prevent coolant boiling and partial fuel melting in the reactor. In the liquid  $D_2O$  loop, a step increase of 0.006 k causes transient boiling in the fuel assembly. Within one second, the temperature of the  $D_2O$  from the fuel assembly rises to the saturation temperature and the  $D_2O$  begins to boil. The magnitude of the pressure increase that results from the steam accumulation has not been established, but it may be great enough to break the rupture disc. This would be a minor consequence, however, when compared to the partial melting of some of the fuel elements in the HWCTR.

A step reactivity increase of 0.004 k can be tolerated by both reactor and test loop. The loop pressure remains at least 300 psi higher than the  $D_2O$  vapor pressure throughout the transient, and boiling does not occur in the loop.

If two control rods are driven out of the reactor simultaneously at maximum speed of about 2.5 ft/sec, the maximum rate of addition of reactivity is about 0.0003 k/sec. As shown in DP-383<sup>(1)</sup>, this accident is self-limiting in the reactor, and reliance need not be placed on fast action by the safety system. The consequences are also mild for the test loop; the D<sub>2</sub>O in the loop does not boil and rupture of the seal between the loop and the reactor is not a threat.

#### 4. Transients Following Loss of H<sub>2</sub>O Flow

Figure 3 shows the temperature and pressure transients that follow a sudden loss of H<sub>2</sub>O flow to the loop heat exchanger. It was assumed in computing these transients that the reactor is scrammed immediately. The further assumption was made that the heat transfer in the heat exchanger instantly decreases to zero as a result of film boiling of H<sub>2</sub>O in the tubes. An alternative assumption is that the heat transfer is unaffected until the H<sub>2</sub>O in the tubes reaches 100°C, at which time the H<sub>2</sub>O is promptly expelled and the heat transfer is nil. The actual situation must lie somewhere between these extremes. The transients are calculated to be very similar for these two cases. It is therefore concluded that the simpler assumption of immediate loss of cooling (Figure 2) is adequate. The seal between the loop and the reactor is not ruptured in either case.

If a scram does not result from the loss of H<sub>2</sub>O flow to the loop, the reactor will continue to operate at 50 MW, and the temperatures and pressure in the loop will increase gradually. These transients are milder than those computed for the original loop design. The reason is that relocation of the surge tank to the downstream side of the loop heat exchanger furnishes a reservoir of cooler D<sub>2</sub>O, which retards the temperature rise following a loss of loop cooling. Immediate rupture of the loop-reactor seal is not a threat in the modified loop even if the reactor is not scrammed immediately. With the original design, the seal would have burst and the loop D<sub>2</sub>O would have boiled into the reactor within about 35 seconds after the loss of H<sub>2</sub>O flow (see DP-465). Of course, if the reactor is not shut down within one or two minutes, the same situation will also occur in the modified loop.

#### 5. Transients Following an AC Power Failure

If the AC power supply to the loop circulating pump fails, the coolant circulation decreases gradually because of the flywheel action to the flow that can be maintained by the emergency DC power. The D<sub>2</sub>O flow was assumed to decrease linearly to one-third of its initial value in 30 seconds, and then to remain constant. Loop transients following such a reduction in D<sub>2</sub>O flow and a subsequent reactor scram are shown in Figure 4. In this instance, the rupture disc between the loop and reactor gas system remains intact.

If the AC power failure does not result in a reactor scram, the reactor will continue to operate at 50 MW. In 30 seconds, the loop pressure and the D<sub>2</sub>O vapor pressure are equal, and the D<sub>2</sub>O begins to boil. There is, however, ample time to scram the reactor manually before the seal between the loop and the reactor is broken.

#### 6. Transients Following Changes in Heat Exchanger Bypass Flow

If the fraction of total D<sub>2</sub>O flow that passes through the heat exchanger is increased linearly from 10 to 100% over a period of 5 seconds at a constant reactor power of 50 MW, the temperatures and pressure in the loop decrease as shown in Figure 5. It is seen from this figure that the decrease in loop pressure is not great enough to break the "low pressure" seal between the loop and the reactor.

If the fraction of total D<sub>2</sub>O flow that passes through the heat exchanger is decreased linearly from 10 to 1% in 5 seconds at a reactor power of 50 MW, the temperatures and pressure in the loop increase as shown in Figure 6. Up to 35 seconds after the start of this increased bypassing of the heat exchanger, the loop D<sub>2</sub>O does not boil. However, it is evident from Figure 6 that the seal between the loop and the reactor will burst within another 5 seconds if corrective action is not taken. If the seal bursts, some of the D<sub>2</sub>O in the loop will flash into the reactor as the loop pressure is relieved. Actually, the reactor would be scrammed in about 17 seconds by the 5°C increase in D<sub>2</sub>O temperature at the outlet of the fuel assembly in the loop. A scram at this time should prevent rupture of the disc.

#### C. MOCKUP OF BAYONET FOR BOILING LOOP

Construction of a full-scale mockup of the bayonet for the boiling loop of the HWCTR was completed, and facilities were installed for flow studies with steam-water mixtures. The objectives of the mockup studies are (1) to determine whether damaging vibration is likely to occur in the bayonet, (2) to establish the effectiveness of the steam quencher in the boiling loop, and (3) to measure the pressure drop due to two-phase flow in the piping between the bayonet and the quencher. Preliminary operation of the mockup indicates that the vibration problem probably will not be serious in the HWCTR bayonet.

The test facility is located in a powerhouse, where steam and water at conditions required for flow testing are available. The mockup of the bayonet is shown in Figure 7, and a flow diagram of the experimental system is presented in Figure 8. Boiler feedwater at a temperature as high as 260°C is introduced into the lower side connection of the bayonet at a nominal flow of 38,000 lb/hr. The water passes down the annulus between the outer housing tube and the fuel enclosure and then flows upward over a bundle of 19 dummy fuel rods. Saturated steam at about 280°C and at a nominal flow of 7,500 lb/hr is dispersed into the upflowing water through multiple small orifices in the walls of each of the dummy

fuel rods. Steam is supplied to the rods by a flexible steel hose and plenum located at the bottom of the test assembly. The steam-water mixture (14% steam quality) is discharged at 270°C from the bayonet assembly through the upper side connection; the mixture is then passed through piping and a quencher that are dimensionally identical with those proposed for the HWCTR boiling loop. Water at 130°C and at a rate of 21,000 lb/hr is supplied to the quencher for condensing the steam. The above flows and temperatures correspond to the nominal design conditions proposed for the HWCTR bayonet. Other operating conditions, as shown in Table I, will also be employed during the mockup tests.

The bayonet mockup and the dummy fuel rods are constructed of carbon steel. All tubular components of the mockup are the same nominal diameter and length as those currently planned for the HWCTR bayonet. The wall thickness of the tubing is also the same except for the steel tubing that simulates the Zircaloy section of the outer housing tube of the HWCTR bayonet. In the mockup, steel tubing with one-half the wall thickness of the Zircaloy tubing was used in order to obtain the same stiffness as in the HWCTR bayonet. The dummy fuel rods (Figure 9) simulate a fuel assembly of 19 oxide rods for irradiation in the HWCTR; the mechanical design of this assembly was described in DP-485. As discussed above, steam is dispersed into the bayonet through orifices in the wall of each dummy rod. The orifices, 124 holes of 1/16-inch ID, are grouped along the length of each rod so as to simulate a cosine heat generation. A 25% radial flux dip is simulated by flow restrictors at the steam inlet ends of the inner rods of the bundle. The side connections and nozzles of the mockup are dimensionally identical with those of the HWCTR. The nozzles are welded into a 5-inch-thick steel bar (Figure 10) that simulates the attachment of the nozzles to the wall of the HWCTR vessel. The test bayonet assembly is enclosed in a 10-inch-diameter tank to protect personnel. If significant vibration is observed in the bayonet mockup, the tank can also be filled with water to reproduce the damping effect of moderator in the HWCTR vessel. The reactor shields in the HWCTR are also simulated in the tank. Vibration of the bayonet mockup can be seen through portholes in the wall of the tank.

In a preliminary experiment that was conducted before the heat exchangers were installed, 4,100 lb/hr of superheated steam at 430°C and 850 psia was dispersed into water flowing into the bayonet at 22,000 lb/hr. Vibration of the bayonet could not be detected visually. The inlet water temperature was 220°C, and the effluent contained 14 wt % steam at 265°C. Although the test was conducted at less than nominal steam flow, it was considered to be a conservative test because the steam was superheated and the subcooling of the inlet water was greater than that expected in the HWCTR. Bayonet startup conditions were included in this test.

#### D. LEAK TESTING OF BAYONET JOINTS

The average rate of H<sub>2</sub>O leakage from a "Conoseal" joint for 2-1/2 inch pipe was well within the design maximum of 40 lb/yr during 94 cycles of a 98-cycle test. For 89 cycles, the leakages throughout each cycle were within the design specification, but in the cooling phases of the 90th to 94th cycles there were 5- to 10-minute pulses of leakage that exceeded the 80 lb/yr range of the moisture-detecting instrument. Beginning with the 95th cycle, the cooling-phase leakage was high enough to be visible as a liquid stream, and the test was terminated. The leakage rates during the first 94 cycles were as follows:

	Leakage Rate, lb/yr of H <sub>2</sub> O			
	Avg. During Test	Heating Phase	Hot Phase	Cooling Phase
Average	1.5	2.1	0.8	2.5
Maximum	-	30	10	80
Minimum	-	0.03	0.02	0.04

The test joint, shown in Figure 11, is one of two candidate joints for connecting the inlet and outlet D<sub>2</sub>O piping to the HWCTR bayonets (see Figure 7). The joint was to have been exposed to temperature and pressure cycles while being subjected to bending forces that simulate the operating loads on the HWCTR. An air motor, also shown in Figure 11, was provided for this purpose. However, the loading mechanism proved to be defective, and all of the cycles were carried out in the absence of a bending force. In a typical 2-hour cycle, the joint was heated for 30 minutes at 850 psig, maintained at 250°C and 850 psig for 1 hour, and cooled to about 50°C at 850 psig in 30 minutes. At the end of each cycle the internal pressure in the joint was reduced to atmospheric pressure; an external pressure of 100 psig was maintained on the joint during the entire cycle, including the vent period. The initial and final torques on the two bolts of the test joint were 60 ft-lb.

The average leakages from a "Grayloc" coolant-connection joint and from a candidate top-closure joint for the bayonets exceeded the design maximum in the first thermal cycle at the conditions described above. Drawings of the two joints are shown in Figures 12 and 13. The excessive leakage from both joints occurred at the beginning of the cooling phase of the first test cycle. Testing of these joints will be resumed when new gaskets of different design are obtained. The manufacturer of the "Grayloc" joint recommended that a gasket of 410 stainless steel, which is standard for this unit, be substituted for the gasket of 304 stainless steel that was used in the test. A "Flexitallic" spiral-wound gasket of stainless steel and asbestos will be substituted for the flat asbestos gasket originally specified for the top closure. In earlier tests of HWCTR closures, the leakage from "Flexitallic" gaskets was well within design specifications for the reactor.

## E. MECHANICAL JOINTS FOR FUEL HOUSINGS

Pressure tests on sample specimens indicate that a flared joint will provide a satisfactory seal between the Zircaloy housing tubes and the stainless steel end fittings of the HWCTR driver elements. These joints must seal against water leakage at a maximum differential pressure of about 25 psi in the HWCTR. The design of the joint is similar to that of a conventional flared tubing joint (see Figure 14); the 0.030-inch wall of the Zircaloy extrusion is flared 20° and is compressed between the mating surfaces of the end fitting and a stainless steel seal ring. The sealing force is applied by screwing together the end fitting and a backup nut. None of eight joints of this design leaked when a pressure differential of 100 psi was applied.

The next step in evaluations of the joint will be a series of tests to investigate its corrosion resistance.

## II. TECHNOLOGY OF FULL-SCALE REACTORS

### A. PHYSICS STUDIES

#### 1. Boiling-D<sub>2</sub>O-Cooled Power Reactors

##### a. Void Coefficients

Improvements were made in the calculations of the effective void coefficient in fuel assemblies that are cooled by boiling heavy water. In the earlier calculations the void fraction was arithmetically averaged along the length of the fuel assembly. The improved computations include an "effective" void fraction,  $\bar{\epsilon}$ , that is weighted by the square of the neutron flux and is defined as follows:

$$\bar{\epsilon} = \frac{\int_0^L \epsilon(x) \phi^2 dx}{\int_0^L \phi^2 dx} \quad (1)$$

where  $\epsilon(x)$  = void fraction at position  $x$  along the assembly length

$$= \frac{\rho_0 - \rho_x}{\rho_0}$$

$\rho_0$  = density of liquid D<sub>2</sub>O at 20°C

$\rho_x$  = density of the steam-water mixture at position  $x$  along the assembly length

$\phi$  = neutron flux, which was assumed to be distributed as a chopped cosine.

$L$  = length of the assembly

Equation (1) was used to compute the effective void fraction,  $\bar{\epsilon}$ , as a function of the exit steam quality at a pressure of 750 psia for several values of inlet subcooling. The results of these calculations are shown in Figure 15.

The change in reactivity associated with a change in effective void fraction is equal to  $\Delta\bar{\epsilon}$  multiplied by the total coolant worth. The total coolant worth is defined as the reactivity change produced by removing all the coolant from an assembly that initially contains liquid  $D_2O$  at  $20^\circ C$ . The change in effective void fraction,  $\Delta\bar{\epsilon}$ , due to a 1% increase in reactor power under conditions of constant coolant flow was computed from Figure 15 and the relationship between exit quality and reactor power. Figure 16 gives the results of these calculations.

The positive void coefficients that were calculated earlier (DP-475) for the Sargent & Lundy fuel element design (uranium oxide rods)<sup>(2)</sup> and for the du Pont fuel design (uranium metal tubes)<sup>(3)</sup> are somewhat smaller than those calculated by the present method. The previously used linear average for the effective void fraction along the fuel length resulted in a calculated void coefficient of  $+1.4 \times 10^{-5}$  k per percent change in power for the oxide assembly; the flux-weighted average resulted in a coefficient of  $+1.8 \times 10^{-5}$  k per percent change in power. Similarly, larger values of the positive void coefficient of the metal tube assemblies were computed by the revised method:  $+9.3 \times 10^{-5}$  versus  $+4.8 \times 10^{-5}$  k per percent power change. Both the old and the new sets of estimates of the void coefficient were computed from a calculated coolant worth of  $+2.8\%$  k for the metal fuel design and  $+0.6\%$  k for the oxide fuel design.

#### b. Power Coefficient of Boiling $D_2O$ Reactors Fueled with Oxide Tubes

In DP-505, it was shown that a uranium-metal-fueled boiling- $D_2O$ -cooled power reactor operating on a direct steam cycle would probably be unstable because of its positive net power coefficient and that the best application for uranium metal tubes would probably be in liquid-cooled power reactors. Fuel elements consisting of a nest of tubes of uranium oxide are being developed as alternatives to the metal fuel elements in the boiling- $D_2O$ -cooled reactor designs. Calculations performed this month showed that if the oxide tubes were about 0.3 inch thick or thicker, the boiling  $D_2O$  reactor would probably be stable. This article discusses the net power coefficients of boiling- $D_2O$ -cooled tubular oxide fuels.

The coefficient of reactivity associated with the oxide fuel temperature was computed. In these calculations (a) the Doppler coefficient was computed by the method of Rosen<sup>(4)</sup>, (b) the fuel temperatures were defined with the data of Hedge<sup>(5)</sup> for the thermal conductivity of uranium oxide, and (c) the effective fuel temperature was taken to be the statistically weighted average temperature throughout the pile for an unflattened flux distribution. The calculated values of the negative fuel coefficients are plotted as solid lines in Figure 17.

The reactor system in which the oxide fuel tubes were placed was assumed to have an exit steam quality of 30%, a maximum heat flux of 200,000 pcu/(hr)(ft<sup>2</sup>), an inlet subcooling of 33°C, and a coolant pressure of 750 psi. These conditions correspond to those of the earlier du Pont design<sup>(3)</sup> of a boiling-D<sub>2</sub>O-cooled power reactor with the exception that the oxide tubes have been substituted for the metal tubes. In the calculations of the coefficients of reactivity associated with coolant voids in this oxide-fueled system, the total coolant worth in the fuel assemblies was assumed to be 1% k and the resonance escape probability to be 0.88. Calculated values of the positive void coefficients for 33 and 10°C inlet subcooling are shown as dashed lines in Figure 17.

The region shown in Figure 17 in which the positive void coefficient exceeds the negative fuel coefficient is a region of instability. Figure 17 shows that if the oxide tubes were thinner than about 0.3 inch, there would be a range of operation, at powers below design power, in which the net power coefficient would be positive and the reactor would not be stable. In such instances the relatively low fuel temperatures would not provide a sufficiently negative effect through the fuel temperature coefficient to override the positive reactivity effects of the voids.

It should be pointed out that the above calculations are subject to large uncertainties because the uncertainties in the coolant worths, the Doppler coefficient, and the thermal conductivity of UO<sub>2</sub> are all very large. In order to define more clearly the regions of instability, experimental measurements to obtain improved values of the above parameters are needed.

## 2. Neutron Slowing-Down Distribution

The major uncertainties in the calculation of the reactivities of candidate power reactor lattices of natural uranium in heavy water lie in the calculation of the resonance escape probability, p. The calculational method most commonly used at the Savannah River Laboratory for this parameter is an elaboration of one proposed by Critoph<sup>(6)</sup> in which resonance capture is assumed to take place at a single energy and in which the neutron distribution at that energy is calculated from a double Gaussian fit to the measured slowing-down distribution from a point fission source. An excellent test of this method is provided by experiments with single fuel assemblies. Measurements of the neutron slowing-down distributions from these assemblies test the applicability of the double Gaussian in practical cases, and measurements of the self-resonance capture test a particularly simple case of the over-all theory. Such measurements have been made in the Process Development Pile (PDP) at the Savannah River Laboratory, and the results are being analyzed. The progress to date is reviewed in the following paragraphs.

The PDP measurements were made with the special loading that was described in the April report, DP-495. In this loading the central

core of the reactor to a diameter of approximately 8 feet is filled only with D<sub>2</sub>O. An outer driver lattice consisting of seven-rod clusters of natural uranium metal on a 14-inch spacing in D<sub>2</sub>O surrounds the central D<sub>2</sub>O core. As shown in the April report, the flux at the center of the D<sub>2</sub>O core is highly thermalized. If a test fuel assembly were located in this position, fissions would be initiated in the fuel assembly with a minimum background of epithermal neutrons.

Five different fuel assemblies were placed individually at the center of the D<sub>2</sub>O core: (a) a single one-inch diameter rod of U<sup>235</sup> in aluminum, (b) a single one-inch diameter rod of natural uranium metal, (c) a cluster of 3, 7, and 19 one-inch diameter natural-uranium rods. The neutron slowing-down distributions resulting from fissions in these assemblies were measured by activating 1/2-inch-diameter foils of indium, gold, and tungsten covered with 0.020-inch-thick cadmium. These materials are all characterized by a predominant neutron absorption resonance and to a first approximation measure the neutron flux distributions at energies of 1.46, 4.91, and 18.8 ev, respectively. U<sup>238</sup> foils, covered with cadmium and with cadmium and uranium, were also used to measure the slowing-down distribution resulting in U<sup>238</sup> resonance captures.

The results of the measurements are shown in Figures 18 and 19. Figure 18 shows the indium-measured fluxes for the different types of fuel assemblies. Figure 19 shows the fluxes measured with foils of indium, gold, tungsten, and U<sup>238</sup> for the enriched fuel rod.

Attempts were made to fit the measured flux distributions,  $\phi(r)$ , to a line-source double Gaussian of the form

$$\phi(r) = \frac{A}{\tau_1} e^{-r^2/4\tau_1} + \frac{B}{\tau_2} e^{-r^2/4\tau_2} \quad (1)$$

where the ordinary neutron age,  $\tau$ , is given by

$$\bar{\tau} = \left[ \frac{A}{A+B} \right] \tau_1 + \left[ \frac{B}{A+B} \right] \tau_2 \quad (2)$$

and  $\tau_1$  = "age" of fast neutrons  
 $\tau_2$  = "age" of epithermal neutrons  
 $r$  = distance from neutron source  
A, B = constants

These attempts were generally unsuccessful because the double Gaussian form seems to give too low a flux at distances beyond about 50 cm from the source. The errors are particularly marked when the present

line-source distributions are compared with the corresponding point-source distributions<sup>(7)</sup>. For the latter, it was found that at large distances the flux should be distributed according to the following expression rather than a double Gaussian.

$$\phi(r) = \frac{e^{-r/\lambda}}{r^2} \quad (3)$$

The term  $\lambda$  is derived from the slope of the  $Ar^2$ -vs.- $r$  curve as shown in DP-163<sup>(7)</sup> and DP-505;  $A$  is the corrected foil activity. An expression similar to Equation (3) presumably should be used for the line source, and work is presently in progress to obtain a better fit of the data.

In addition to the flux distribution measurements in the moderator, measurements were also made with  $U^{238}$  foils directly in the fuel assemblies. By counting the 104 kev X-ray line in the decay of the  $Np^{239}$  produced in the foils and by making measurements with and without cadmium covers on the foils, it was possible to obtain  $\rho$ , the ratio between episcadmium and subcadmium radiative captures in  $U^{238}$ . The results of this measurement are given in Figure 20. These results are now being used to obtain values of self-resonance captures,  $1 - \rho$ , as described in DP-505. They will then be compared with calculated values of the self-resonance captures as a test of the calculational methods now used.

### 3. The (n,2n) Reaction with Deuterium

The (n,2n) reaction with deuterium and the (n, $\alpha$ ) and (n,p) reactions with oxygen have been ignored in past calculations of the physics characteristics of  $D_2O$ -moderated reactors because of insufficient data to permit accurate prediction of the effects of these reactions. However, recent measurements<sup>(8)</sup> of the (n,2n) cross section of deuterium by Hill, Goldberg, LeBlanc, and Taylor at the Lawrence Radiation Laboratory give results in good agreement with theory<sup>(9)</sup> and permit reasonably accurate calculations to be made of the effect of this reaction on the multiplication factor of heavy-water-moderated reactors. Multigroup calculations were made for an infinite volume of  $D_2O$  containing a uniformly distributed source of fission neutrons to determine the effects on neutron economy of the (n,2n) reaction and the (n, $\alpha$ ) and (n,p) reactions with oxygen. The calculations show that the effects of these reactions almost cancel each other; there is a net loss of 0.06 neutron per 100 fission neutrons.

In the multigroup calculation all groups had the same width of lethargy band, 0.1 lethargy unit, where the lethargy,  $u = \log 10/E$  and the neutron energy  $E$  is in Mev. The highest energy group was assumed to have an upper bound of 14.9 Mev. The tabulation of the fission spectrum<sup>(10)</sup> given in Reference (11) was employed. Oxygen cross section and anisotropic scattering data were taken from Reference (12). Legendre polynomial fits

to the available data for deuterium<sup>(13-17)</sup> were employed to express the anisotropic scattering data in the same form as that for oxygen in Reference (12), with weight given to what appear to be the best data.<sup>(13,14,17)</sup> The calculations show that per fission neutron there are 0.00414 (n,2n) reactions with deuterium, 0.00472 (n, $\alpha$ ) and (n,p) reactions (mainly n, $\alpha$ ) with oxygen, and 0.00097 inelastic collisions with oxygen. The net loss of neutrons per fission neutron is thus 0.00058. The (n,2n) effect is somewhat larger than stated by Weinberg and Wigner<sup>(18)</sup>, but much smaller than would be calculated from the cross sections assumed by Howerton<sup>(19)</sup> or Emmerich<sup>(20)</sup>.

## B. REACTOR FUELS AND MATERIALS

### 1. Fuel Elements of Uranium Metal

#### a. Thin-Walled Coextruded Tubes

The development of fabrication techniques for thin Zircaloy-clad tubes of uranium metal for irradiation testing continued to receive primary attention at Nuclear Metals, Inc., during this report period. Evaluation was completed for the three tubes of unalloyed uranium that had been extruded in April with the billet cores having identical "angular" preshaped end plugs. As reported last month in DP-505 from preliminary examination of one of these tubes, only near the rear outside surface were the flow shapes at the core ends entirely satisfactory; the end tapers produced some clad thinning at the front outer surface and at both the front and rear inner surfaces. However, in spite of the slight thinning of the clad, these tubes are generally considered to be of good quality. Two of the tubes, each approximately 10 feet long, have been processed for flow testing and irradiation, respectively, and shipped to Savannah River. The third tube, which is about 4 feet long and typical of those intended for irradiation in the VBWR, was destructively examined.

An additional eight tubes have been extruded and partially evaluated in the experimental program seeking to develop improved billet end shapes. One of the modified designs resulted in a tube meeting the desired minimum cladding thickness. Still further improvement of the cladding uniformity at the end tapers is being sought. Another experiment is now in progress.

Short, thin-walled tubes with enriched cores of unalloyed uranium, U - 1 wt % Si, and U - 1.5 wt % Mo are to be irradiated in the VBWR. Complete evaluation of a natural-uranium prototype tube of the silicon alloy revealed virtually no thinning of the cladding at the core end tapers, nor other deviations from desired characteristics. An enriched tube having the same billet design was extruded and processed for shipment to Vallecitos. This tube is well within specifications; the uniform core section is about 3<sup>4</sup>/<sub>8</sub> inches long, and front and rear tapers are 4-1/8 and 3-5/8 inches long, respectively.

The thin-walled natural-uranium prototype tube of the U - 1.5 wt % Mo alloy had an excessive amount of clad thinning. The cladding on the inner surface at the rear end taper was about 0.005 inch thinner than the specified minimum. Further prototype tubes of this alloy and of unalloyed uranium will be designed.

## 2. Fuel Elements of Uranium Oxide

### a. Swaged Tubes Clad with Zircaloy

Zircaloy-clad,  $UO_2$  fuel tubes have been fabricated at Savannah River Laboratory for irradiation testing. Ten tubular assemblies of  $UO_2$  were compacted by vibration to approximately 72% of theoretical density and then swaged to approximately 91% of theoretical density. Eighteen specimens, each approximately 2 feet long, were fabricated from these tubes and evaluated. Six of the specimens were delivered for irradiation in a Savannah River reactor.

In the fabrication of these tubes, vibratory compaction was used to obtain a preselected oxide density before swaging. The OD of the Zircaloy-2 outer sheaths was 2.50 inches; the assemblies were to be swaged to a final diameter of 2.295 inches in order to fit into available housing tubes. These conditions restricted the reduction in area during swaging to 24%. In order to produce a core density in excess of 90% of theoretical density during swaging and to minimize cladding strain, it was necessary to load the assemblies to an initial density of about 72% of theoretical. The desired loaded density was obtained by using a particular blend of Spencer fused oxide and a particular setting on the vibratory compactor. The blend consisted of 10% by weight of -10, +16 mesh, 80% of -20 mesh, and 10% of -200 mesh. The setting on the vibratory compactor was chosen to yield the desired packing density rather than the maximum density obtainable with the particular oxide blend.

Swaging was carried out in seven passes. The reduction was less than that given earlier tubes that were sheathed with stainless steel. The outer and inner Zircaloy sheaths were reduced in area 14 and 18%, respectively. The 2-foot-long specimens were evacuated and then filled with helium before the permanent end plugs were welded in place.

In general, the surfaces of the Zircaloy-clad tubes were better than those of earlier tubes that had experienced greater reductions. Although the surfaces generally showed less roughening due to oxide penetration, the maximum penetration was larger because of the larger size of oxide particles that were used. The maximum penetration was as great as 0.009 inch. The outer and inner surfaces of the outer sheath were both good. The inner sheaths, however, were scored during removal of the mandrels. This scoring, which is believed to be due to lubrication breakdown, ranged from slight to moderate; the extent of the damage is being determined. The sheath thickness averaged about 0.030 inch; the minimum sheath thicknesses are being determined on evaluation specimens.

## b. Uranium Metal Impurity in Fused Uranium Oxide

A one-ton order of uranium oxide fused by an outside supplier contained small amounts of uranium metal, perhaps as much as 1 or 2%. There is some concern over this impurity because little is known about the effect of such an impurity on the in-pile behavior of  $UO_2$ . The existence of a second phase within the fused  $UO_2$  is shown clearly in Figure 21. The unknown phase was positively identified as alpha uranium by a special X-ray diffraction technique. An earlier order of fused  $UO_2$  from the same vendor did not contain this second phase of metallic uranium. Discussions with the vendor indicate that the uranium can be kept out of the fused  $UO_2$  by proper control of the fusion operation and will be eliminated from future orders.

## 3. Cladding Studies

### a. Development of Zirconium Cladding Alloys

One of the factors affecting the exposure lifetime of a uranium metal fuel element is the in-pile ductility of the Zircaloy cladding. If the ductility can be improved, the frequency of fuel element failures should be decreased. Since tin is the primary cause of the higher strength of Zircaloy-2 over unalloyed zirconium, it follows that a reduction in tin content may improve ductility. Very limited data were obtained by WAPD and KAPL several years ago on the irradiated tensile properties of such an alloy, Zircaloy-3. These data show no change in the reduction-of-area value for Zircaloy-3 in contrast to a decrease of approximately 25% for Zircaloy-2.

A program has been initiated to re-evaluate the ductility of Zircaloy-3. Laboratory-scale ingots are being prepared by Harvey Aluminum, Inc. for fabrication and tensile testing at room temperature, 250°C, and 350°C. These ingots will have oxygen contents of 660 and 1000 ppm, which is significantly less than in the Zircaloy-3 tested by WAPD and KAPL. Control ingots of Zircaloy-2 are also being made for comparison purposes.

Tensile specimens of both the Zircaloy-3 and Zircaloy-2 control material will be prepared for irradiation at Savannah River and evaluation of postirradiation ductility.

Corrosion testing of these alloys will be done at Harvey Aluminum, Inc.

### b. Swaged Cladding

An examination is underway to determine the cause of rupture in the swaged tube of stainless-steel-clad oxide that failed in an SRP reactor (DP-495, DP-505). To date the cause of the failure is still undetermined. Part of the examination is aimed at characterizing the ductility of the stainless steel sheaths after swaging. Tests performed at room temperature show that there is a considerable loss in ductility during swaging;

however, the swaged sheaths are still quite ductile in bending and simple tension. Ring specimens from sheaths that are similar to those used with the irradiation specimens have been slit, opened, and bent double without fracture.

Tensile tests were run on longitudinal strips of swaged sheathing and are reported in the table below. These strips were machined from the outer sheaths of tubular elements that were fabricated at the same time as were the irradiation specimens.

Tensile Properties of Stainless Steel Sheathing

<u>Condition</u>	<u>Yield Strength, psi</u>	<u>Ultimate Strength, psi</u>	<u>Elongation to Fracture, %</u>	<u>Reduction in Area, %</u>
As received (annealed)	42,200	93,200	66	51
	44,400	98,600	73	52
	43,300	95,900	74	51
Swaged <sup>(a)</sup>	107,100	119,200	24	37
	101,400	116,800	26	42
Swaged <sup>(b)</sup>	121,200	131,600	15	25
	116,300	124,400	16	27
	114,600	126,900	19	30

(a) These specimens came from tubes fabricated at the same time as the irradiation specimen that failed.

(b) These specimens came from tubes fabricated at the same time as another oxide assembly that has been performing satisfactorily.

As shown in the above table, swaged sheaths are still ductile in simple tension. Specimens are being prepared for hydrostatic burst tests to study the effect of changing the stress state and strain direction.

#### 4. Zircaloy-to-Stainless-Steel Joints

A development program at Nuclear Metals, Inc., has established the conditions for producing metallurgically bonded stainless-steel-to-Zircaloy tubular joints by tandem extrusion. Fabrication details were given in DP-505. A small lot of 2-inch-diameter joints that appeared to have satisfactory mechanical and corrosion properties for the conditions of intended use, as reactor pressure tubes, provided the demonstration of the working process. A new phase of this program has now been started to demonstrate that larger diameter joints, approximately 3-1/4 inches, can be made and that cold working can be incorporated as the final process step without impairment of the joint quality. Some cold working is desired to enhance the mechanical properties of the Zircaloy tubing.

Eighteen 2-inch-diameter joints have been extruded to provide material for preliminary cold-working experiments. These experiments are to establish the amount of cold work to be applied to the larger diameter joints. Concurrently, work has been started on fabrication of tools and billet components for extrusion of a demonstration set of four 3-1/4 inch diameter joints.

### C. IRRADIATION TESTING

#### 1. Tubes of Uranium Metal

##### a. Unalloyed Uranium Tube in the NRU Reactor

The NRU irradiation test of an unalloyed uranium tube clad with Zircaloy-2 was terminated because of damage done to the fuel element during attempted reinsertion into the reactor E-20 loop. The tube had successfully undergone exposure to a maximum of 950 MWD/T with only 1.5% volume increase and 0.14% outer cladding strain. Detailed postirradiation measurements of the tube and the irradiation test conditions were given in DP-505. The surface quality of the tube was observed to be good and no bow was noticed. Continuation of the test was planned. However, after the attempts at reloading, re-examination of the assembly revealed that (a) the shroud assembly was buckled at several places, (b) the fuel tube was scratched, and (c) the fuel tube had bowed a maximum of about 0.200 inch. Even with redesigned end fittings and a new shroud, the bow was so great that the tube could not be returned to the loop for additional irradiation. No further irradiation testing of metal fuel tubes is currently scheduled at Chalk River.

##### b. Lead-Insulated Uranium Tubes

Further investigation of the causes and means of control of swelling in uranium-base metal fuels during irradiation will be carried out with a series of irradiation tests to correlate volume instability with (1) initial metallurgical structure, and (2) relative transformation rates.

The fuel specimens, uranium-base metal cores clad in Zircaloy-2, are contained in stainless steel capsules, as shown in Figure 22. Insulating layers of lead on the inside and outside surfaces of the fuel tubes permit the attainment of surface and central metal temperatures approximately equal to those of power reactor fuel elements. The stainless steel sheaths of the capsule provide strong secondary containment in case of a failure of the Zircaloy cladding. The capsule is designed to accommodate thermocouples if desired.

Design of an irradiation assembly that will contain twelve capsules is in progress.

## 2. Tandem-Extruded Joints of Zircaloy to Stainless Steel

Three Zircaloy-to-stainless steel tandem-extruded joints are scheduled to be irradiated in the core of a Savannah River reactor. The joints will be mechanically loaded in tension by a loading bolt, as shown in Figure 23, to a stress of about 20,000 psi. The three joints will be contained in a housing and will be cooled by liquid D<sub>2</sub>O flowing at a rate such that the maximum temperature will be less than 90°C. In the core of a Savannah River reactor, the joints will accumulate exposure at a much more rapid rate than they would in a typical D<sub>2</sub>O-moderated power reactor where the joints would be located some distance from the edge of the core. However, the temperature of the test joints will be much lower than would be encountered in power reactor service. After irradiation, the joints are to be visually inspected in a high level cave, and to be mechanically and metallurgically tested for soundness and strength.

### D. ENGINEERING STUDIES

#### 1. Design of Fuel Assemblies Cooled by Boiling D<sub>2</sub>O

In DP-505, results were presented of preliminary calculations of the distribution of coolant in fuel assemblies that are being considered for irradiation in the boiling D<sub>2</sub>O loop of the HWCTR. One of the fuel assemblies for which results were presented is a cluster of 19 rods of uranium oxide. In these calculations, the total cross section for coolant flow through the 19-rod assembly was divided into three discrete regions (i.e., not interconnected). Actually, crossflow of coolant between these regions will occur because of the existence of lateral pressure gradients that result from differences in geometry and heat generation among the regions. More recent calculations indicate that for the 19-rod designs discussed in DP-505, coolant crossflow has little effect on the local exit steam qualities.

To obtain an estimate of the effect of the crossflow on the coolant distribution, a calculational method was developed whereby the pressure drops across 6-inch increments of length of the fuel assembly are matched in the three coolant regions by adjusting individual flows as necessary. Thus, the flow in each region varies along the length of the fuel assembly. The exit steam qualities as computed by this method are compared in Table II with those computed on the basis of no crossflow. It is seen that in these particular designs, the crossflow has little effect on the exit steam qualities.

#### 2. Mechanical Seals for Pumps

Further measurements were made of the vapor leakage from a mechanical seal on a water pump that operates in a flow loop at a suction pressure of 850 psig. Initial results of leakage through this seal, a Borg-Warner

Type "D" design, were reported in DP-505. Subsequently, the faces of the seal were replaced because of indications of imminent failure. During the last 24 hours of operation with the old faces, the vapor leakage was less than 0.02 lb/yr. In the first 20 days of operation with new seal faces, the average vapor leakage was 3.3 lb/yr. The minimum and maximum vapor leakages during this period were 0.02 and 22 lb/yr, respectively. The average liquid leakage rate was 830 lb/yr with the old faces and 2900 lb/yr with the new faces.

Bench-scale tests of the "Durametallic" mechanical seals described in DP-505 were completed. The purpose of these tests, which will be repeated with seals obtained from other manufacturers, is to obtain data on the effects of selected pump operating variables on the water leakage from commercially available mechanical seals. The leakage data are shown in Table IV, and drawings of the seal assembly and the seal tester are shown in Figures 24 and 25, respectively. The leakage collection system was almost identical with that described last month for the seal assembly of the pump discussed above. Two tests were made on both the inboard and outboard seals; shaft speed and pressure were varied in both tests. In the first test only the liquid leakage was measured, but in the second test the vapor leakage from the outboard seal assembly was also measured. The average liquid leakage from the inboard seal varied from 5 lb/yr at 1000 psig and a shaft speed of 3600 rpm to 10,000 lb/yr at 500 psig and 3600 rpm. The average liquid leakage from the outboard seal varied from 0.3 to 21,000 lb/yr under the same conditions. The average vapor leakage from the outboard seal varied from 1 lb/yr at 1000 psig and 580 rpm to 28 lb/yr at 750 psig and 3600 rpm.

The most significant result of the tests is demonstration that at all conditions the vapor leakage, which is not readily recoverable, is extremely low and therefore not of economic importance for power reactors. Inconsistencies and lack of reproducibility in the data of Table III prevent firm conclusions being drawn concerning the variation of liquid leakage with shaft speed and pressure. Nevertheless, a general trend for the leakage to rise with increasing speed or decreasing pressure can be discerned. There is also a very rough proportionality between liquid and vapor leakage.

The "Durametallic" seals have been replaced by Borg-Warner seals, and tests on the latter are now in progress.

## BIBLIOGRAPHY

1. St. John, D. S., et al. Preliminary Hazards Evaluation of the Heavy Water Components Test Reactor (HWCTR). E. I. du Pont de Nemours & Co., Savannah River Lab., Aiken, S. C. DP-383, 181 pp. (May 1959).
2. Design Study - Heavy Water Moderated Power Reactor Plants, Summary, Parts 1, 2, and 3. Sargent and Lundy, Chicago, and Nuclear Development Corp. of America, White Plains, N. Y. SL-1661, 81 pp. (June 1959).
3. Heavy-Water-Moderated Power Reactors - Engineering and Economic Evaluations - Volume I - Summary Report. E. I. du Pont de Nemours & Co., Eng. Dept., - Design Division, Wilmington, Del. DP-510, 119 pp. (June 1960).
4. Blomberg, P., E. Hellstrand, and S. Horner. The Temperature Coefficient of the Resonance Integral for Uranium Metal and Oxide. A.B. Atomenergi, Sweden, RFX-32, 6 pp. (June 22, 1959).
5. Runnalls, O. J. C. "UO<sub>2</sub> - Fabrication and Properties". Nucleonics 17, No. 5, 104-111 (1959).
6. Critoph, E. Comparison of Theory and Experiment for a) Lattice Properties of D<sub>2</sub>O-U Reactors, b) Central Rod Experiments, and c) Foreign Rod Experiments. Atomic Energy of Canada Ltd., Chalk River, Ont. CRPP-655, 65 pp. (July 1956). (AECL-350)
7. Wade, J. W. Neutron Age in Mixtures of Light and Heavy Water. E. I. du Pont de Nemours & Co., Savannah River Lab., Aiken, S. C. DP-163, 35 pp. (June 1956).
8. Reports to the AEC Nuclear Cross Sections Advisory Group. J. A. Harvey, Secretary, Washington, D. C. WASH-1028, 74 pp. (April 1960).
9. Frank, R. M. and J. L. Gammel. "Inelastic Scattering of Protons and Neutrons by Deuterons". Phys. Rev. 93, 463-70 (1954).
10. Cranberg, L., et al. "Fission Neutron Spectrum of U<sup>235</sup>". Phys. Rev. 103, 662-70 (1956).
11. Reactor Physics Constants. Argonne National Lab., Lemont, Ill. ANL-5800, 540 pp. (1958).
12. Lustig, H., H. Goldstein, and M. H. Kalos. An Interim Report on the Neutron Cross Sections of Oxygen. Nuclear Development Corp. of America, White Plains, N. Y. NDA-086-2, 31 pp. (January 1958).

13. Allred, J. C., A. H. Armstrong, and L. Rosen. "The Interaction of 14-Mev Neutrons with Protons and Deuterons". Phys. Rev. 91, 90-99 (1953).
14. Seagrave, J. D. "Recoil Deuterons and Disintegration Protons from the n-d Interaction, and n-p Scattering at  $E_n = 14.1$  Mev". Phys. Rev. 97, 757-65 (1955).
15. Adair, R. K., A. Okazaki, and M. Walt. "Scattering of Neutrons by Deuterons". Phys. Rev. 89, 1165-70 (1953).
16. Wantuch, E. "The Scattering of 4.5- and 5.5-Mev Neutrons by Deuterons". Phys. Rev. 84, 169-72 (1951).
17. Seagrave, J. D. and L. Cranberg. "n-d Scattering at 2.45 and 3.27 Mev". Phys. Rev. 105, 1816-20 (1957).
18. Weinberg, A. M. and E. P. Wigner. The Physical Theory of Neutron Chain Reactors. Chicago: University of Chicago Press, p. 449 (1958).
19. Howerton, R. J. Semi-Empirical Neutron Cross Sections - 0.15-15 Mev - Part II. University of California, Lawrence Radiation Lab., Livermore, Calif. UCRL-5351, 274 pp. (November 1958).
20. Emmerich, W. S. Multigroup Neutron Data for Deuterium. Westinghouse Electric Corp. Research Labs., Pittsburgh, Pa. NP-8363, 15 pp. (September 1958).

TABLE I

PROPOSED TEST CONDITIONS FOR BAYONET MOCKUP

Test No.	Bayonet Effluent Conditions			Water Flow to Bayonet	Steam Flow to Bayonet	Bayonet Effluent, lb/hr	
	Pressure, psia	Temp., °C	Steam Quality, wt %	Temperature, °C	Flow, lb/hr		840 psia, 276°C
1	780	268	10	248	39,200	7,100	46,300
2			10	263	59,500	7,600	67,100
3			10	268	70,600	8,000	78,600
4	780	268	14	239	26,200	7,000	33,200
5			14	258	38,100	7,500	45,600
6			14	263	42,300	7,700	50,000
7			14	268	48,200	7,800	56,000
8	780	268	30	205	9,100	6,400	15,500
9			30	263	17,000	7,700	24,700
10			30	268	18,300	7,800	26,100

TABLE II

EXIT STEAM QUALITIES FOR FUEL ROD CLUSTERS COOLED BY BOILING WATER

Design (a)	Method of Analysis (b)	I		II		III	
		a	b	a	b	a	b
Exit Steam Quality, wt %	Inner Region	39.8	36.2	19.3	19.3	3.8	6.8
	Middle Region	20.1	19.4	22.1	20.1	27.0	23.0
	Outer Region	6.2	7.1	7.1	7.7	8.9	9.2

(a) Design I - 19-rod bundle of 0.55-inch OD rods in 3.2-inch ID housing (See DP-485).

Design II - Design I with no heat generation in the central rod

Design III - Design II with central rod of 0.25 inch in diameter

(b) Methods of Analysis:

a. Flow channels not interconnected - no crossflow

b. Flow channels interconnected - crossflow occurs

Power = 1.43 MW

Flow (H<sub>2</sub>O) = 45,600 lb/hr

Pressure = 795 psia

Subcooling = 9°C

Axial Cosine Flux Distribution

TABLE III

LEAKAGE DATA FROM BENCH TESTS OF "DURAMETALLIC" MECHANICAL SEALS

Shaft Speed, rpm	Pressure, psig	Liquid Leakage, lb/yr						Length of Run, hr	Outboard Seal Vapor Leakage, lb/yr			Length of Run, hr
		Inboard Seal (a)			Outboard Seal (b)				Avg.	Max.	Min.	
		Avg.	Max.	Min.	Avg.	Max.	Min.					
<u>TEST NO. 1</u>												
3600	1000	5	-	-	.3	-	0	27-IB <sup>(a)</sup> 24-OB <sup>(b)</sup>	-	-	-	-
3600	1000	7	-	-	1	-	0	24	-	-	-	-
3600	1000	20	380	0	8	260	0	23-IB 26-OB	-	-	-	-
2500	1000	360	590	260	150	190	40	24	-	-	-	-
1500	1000	120	280	70	70	130	60	24	-	-	-	-
580	1000	50	110	0	6	60	0	24	-	-	-	-
3600	750	1700	2100	1500	400	720	250	24	-	-	-	-
3600	500	2000	2400	1700	1000	1000	680	24	-	-	-	-
3600	250	470	800	320	2700	4400	1800	24	-	-	-	-
<u>TEST NO. 2</u>												
3600	1000	500	650	210	200	240	60	55	7	11	3	19
2500	1000	60	550	0	20	150	0	21	4	10	4	9
1500	1000	10	100	0	20	240	0	51	1	2	1	14
580	1000	50	260	0	2	40	0	92	1	4	0.1	84
3600	750	3100	6400	50	2300	5900	830	184	28	35	10	87
3600	500	10,000	11,000	4600	17,000	21,000	14,000	22	3	27	2	12
3600	250	Leakage exceeded capacity of measuring system							-	-	-	-

(a) Inboard (IB) seal for shaft diameter of 2.00 inches

(b) Outboard (OB) seal for shaft diameter of 2.63 inches

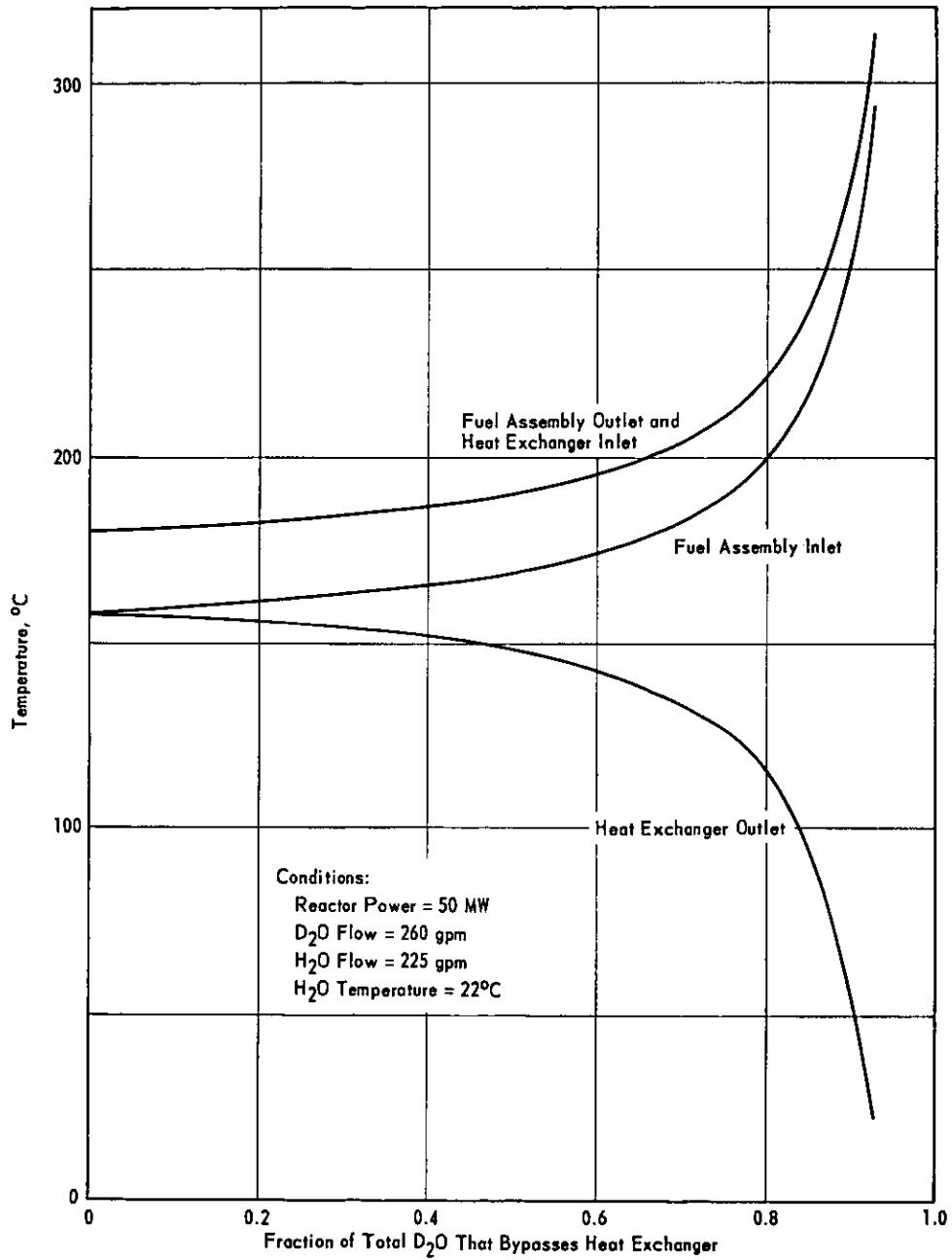


FIG. 1 STEADY-STATE D<sub>2</sub>O TEMPERATURES IN LIQUID D<sub>2</sub>O LOOP OF HWCTR

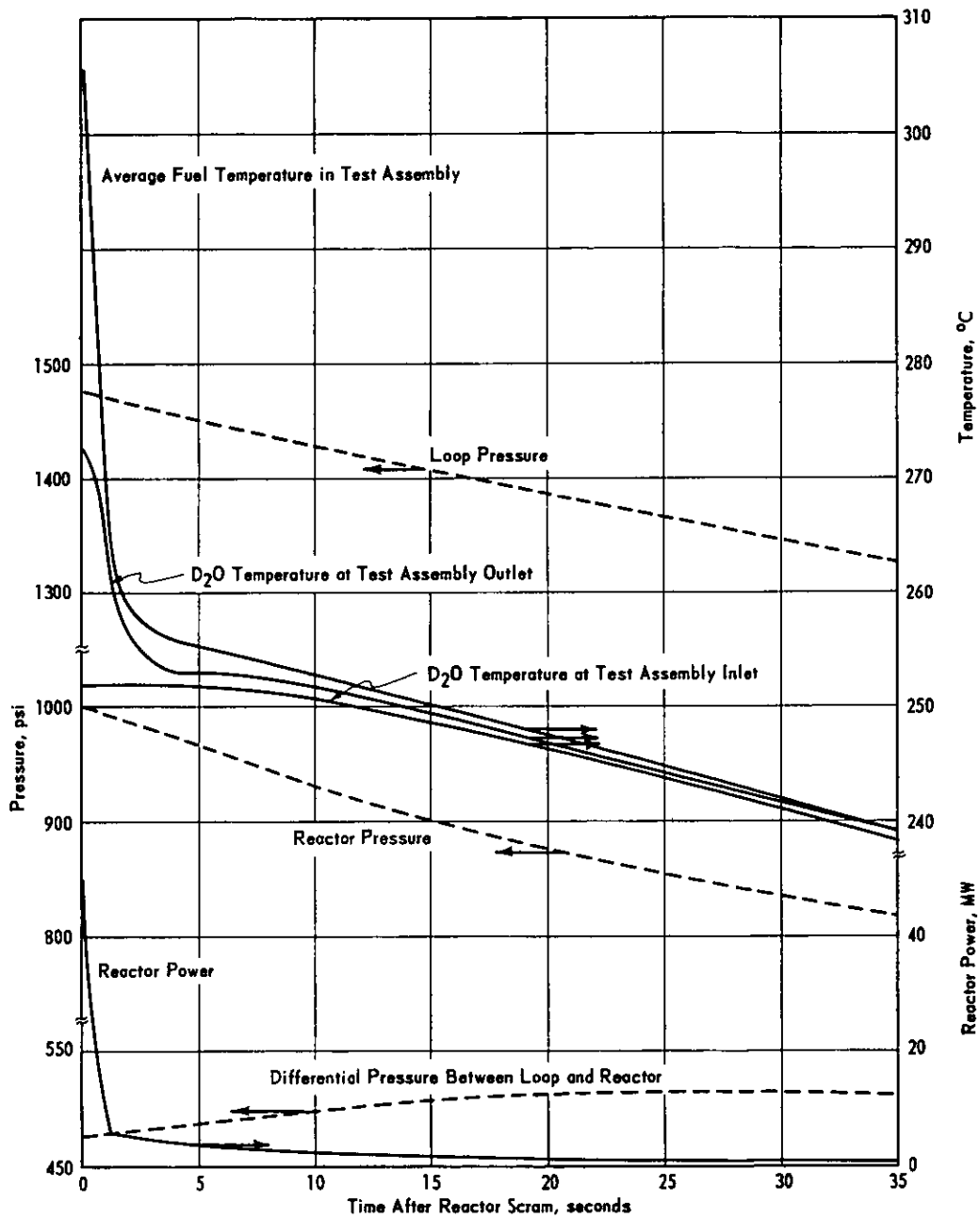


FIG. 2 TRANSIENTS IN LIQUID D<sub>2</sub>O LOOP OF HWCTR AFTER REACTOR SCRAM

Reactor Power = 50 MW

Prompt Temperature Coefficient of Reactivity =  $-2 \times 10^{-5}$  k/°C

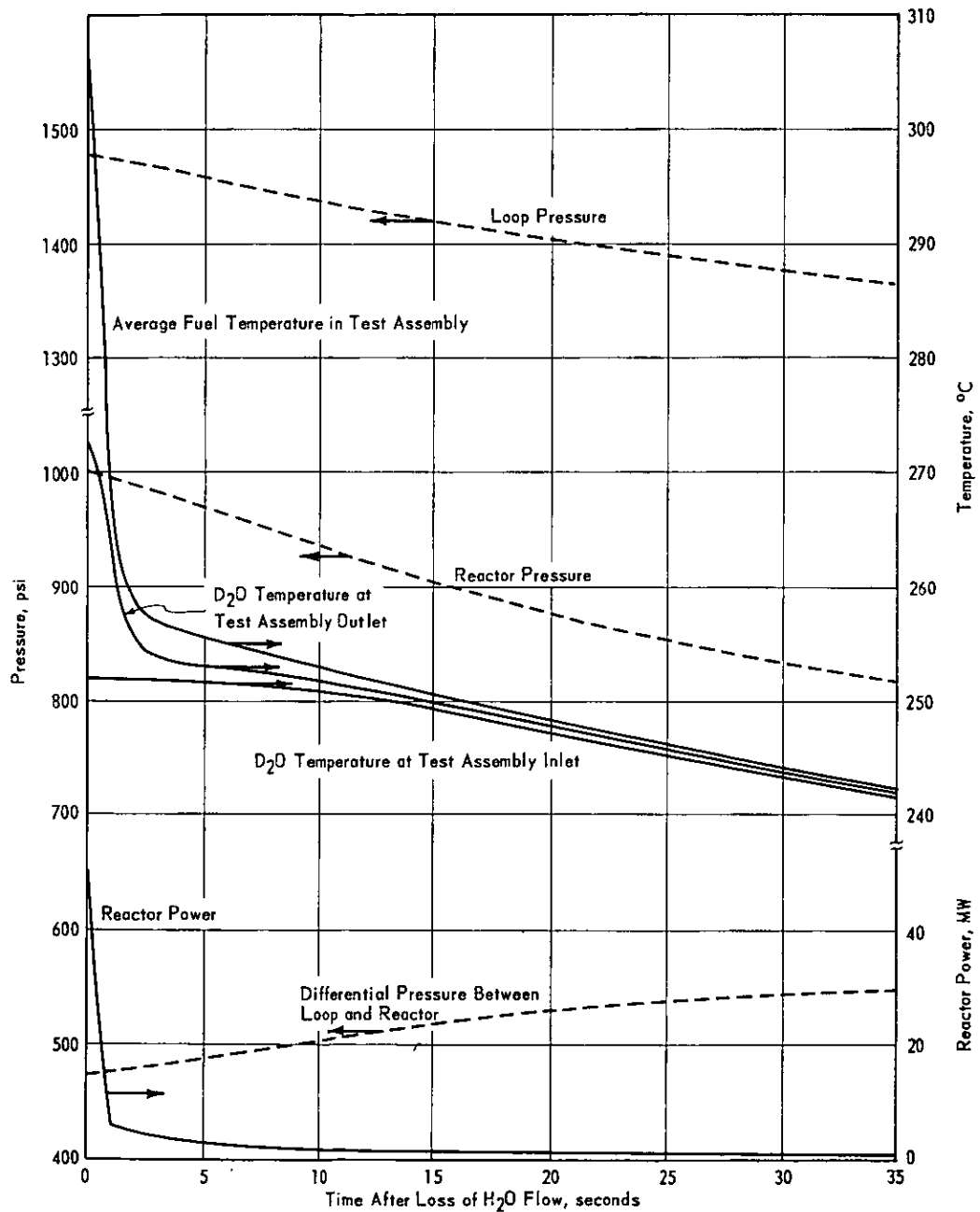


FIG. 3 TRANSIENTS IN LIQUID D<sub>2</sub>O LOOP OF HWCTR AFTER SUDDEN LOSS OF H<sub>2</sub>O FLOW TO LOOP HEAT EXCHANGER

Basis: Reactor scrammed immediately.

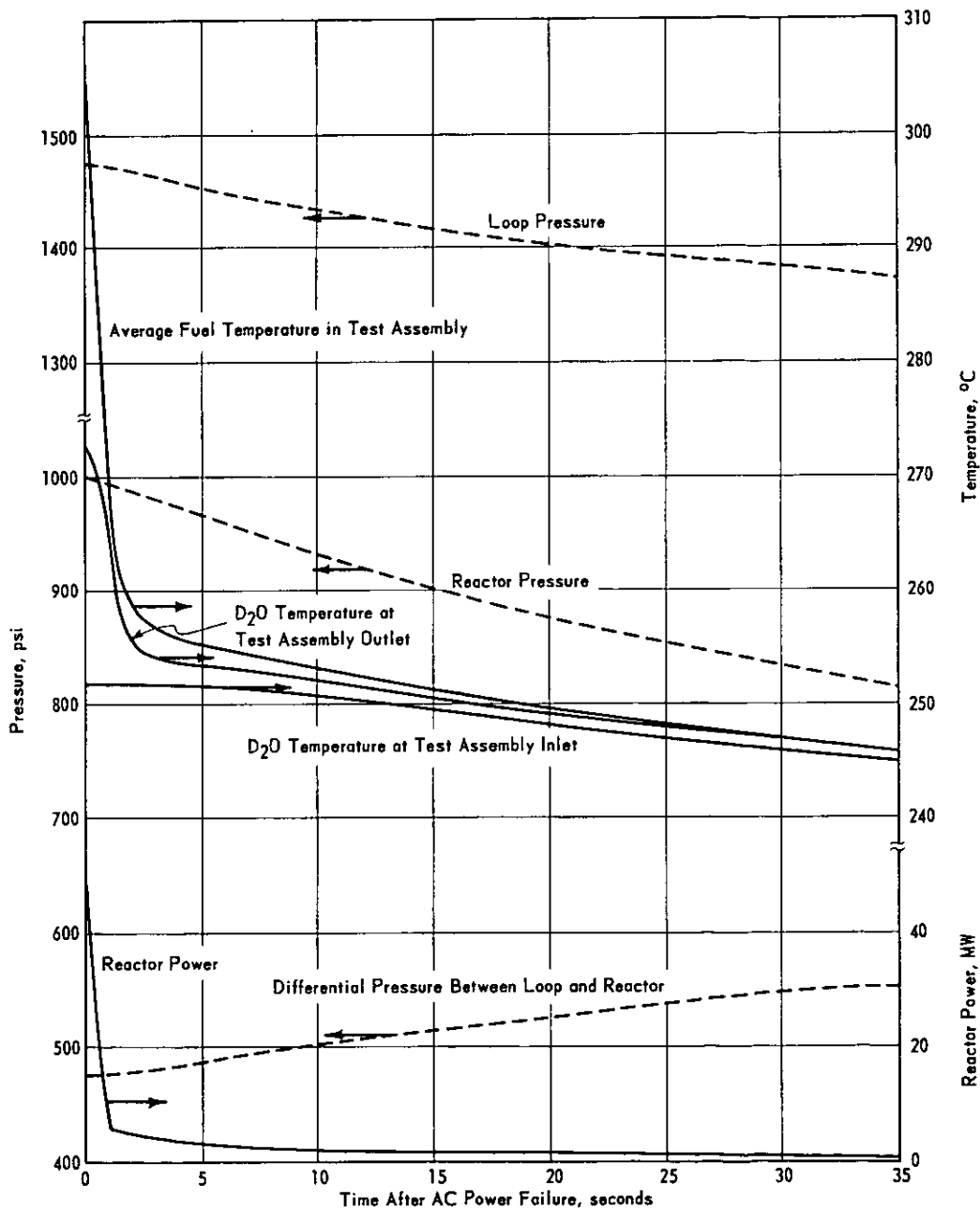


FIG. 4 TRANSIENTS IN LIQUID D<sub>2</sub>O LOOP OF HWCTR AFTER AC POWER FAILURE  
 Basis: Reactor scrammed immediately.

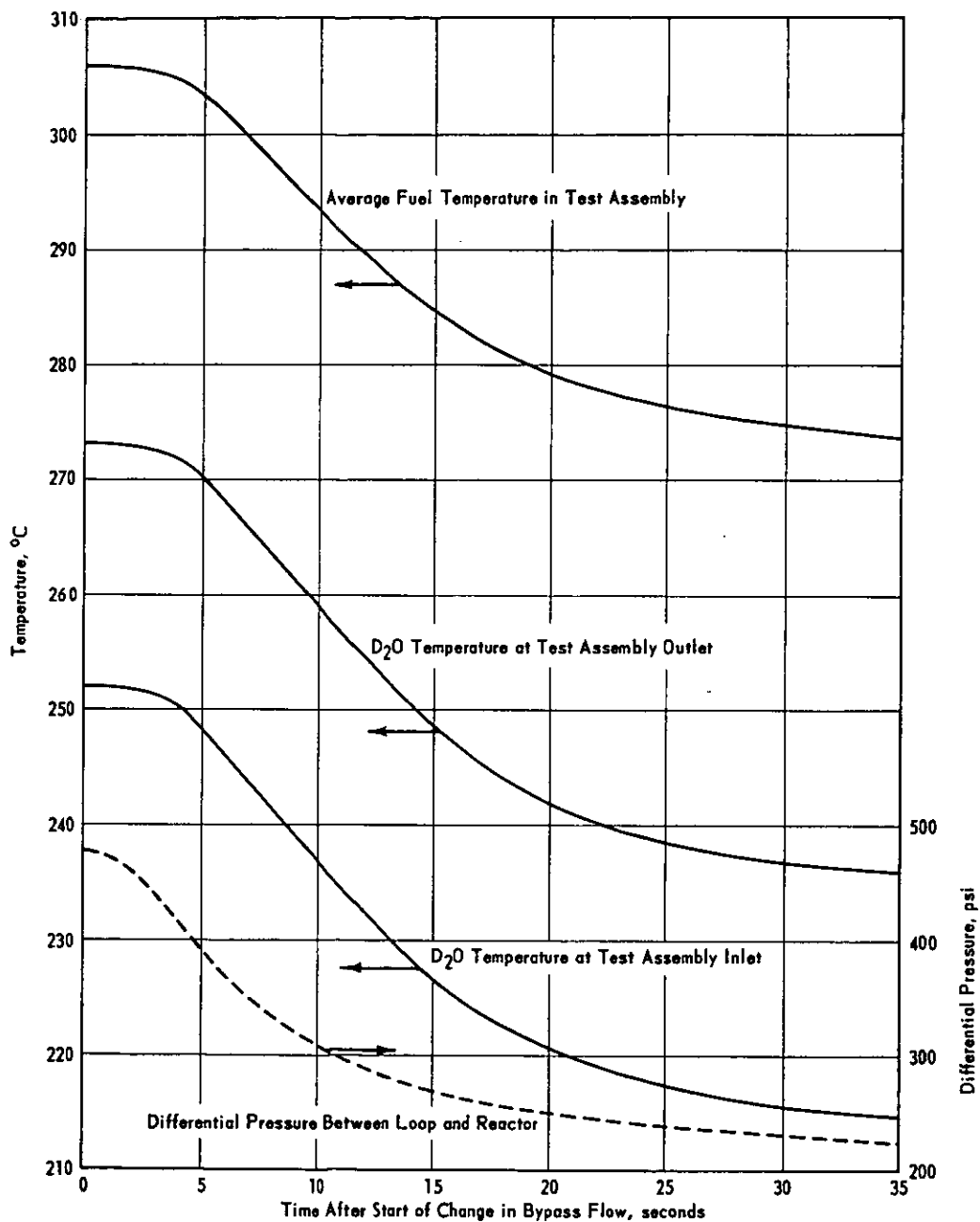


FIG. 5 TRANSIENTS IN LIQUID D<sub>2</sub>O LOOP OF HWCTR AFTER DECREASE IN BYPASS FLOW AROUND LOOP HEAT EXCHANGER

Basis: Bypass flow decreases from 90% of total flow in loop to zero in 5 seconds.

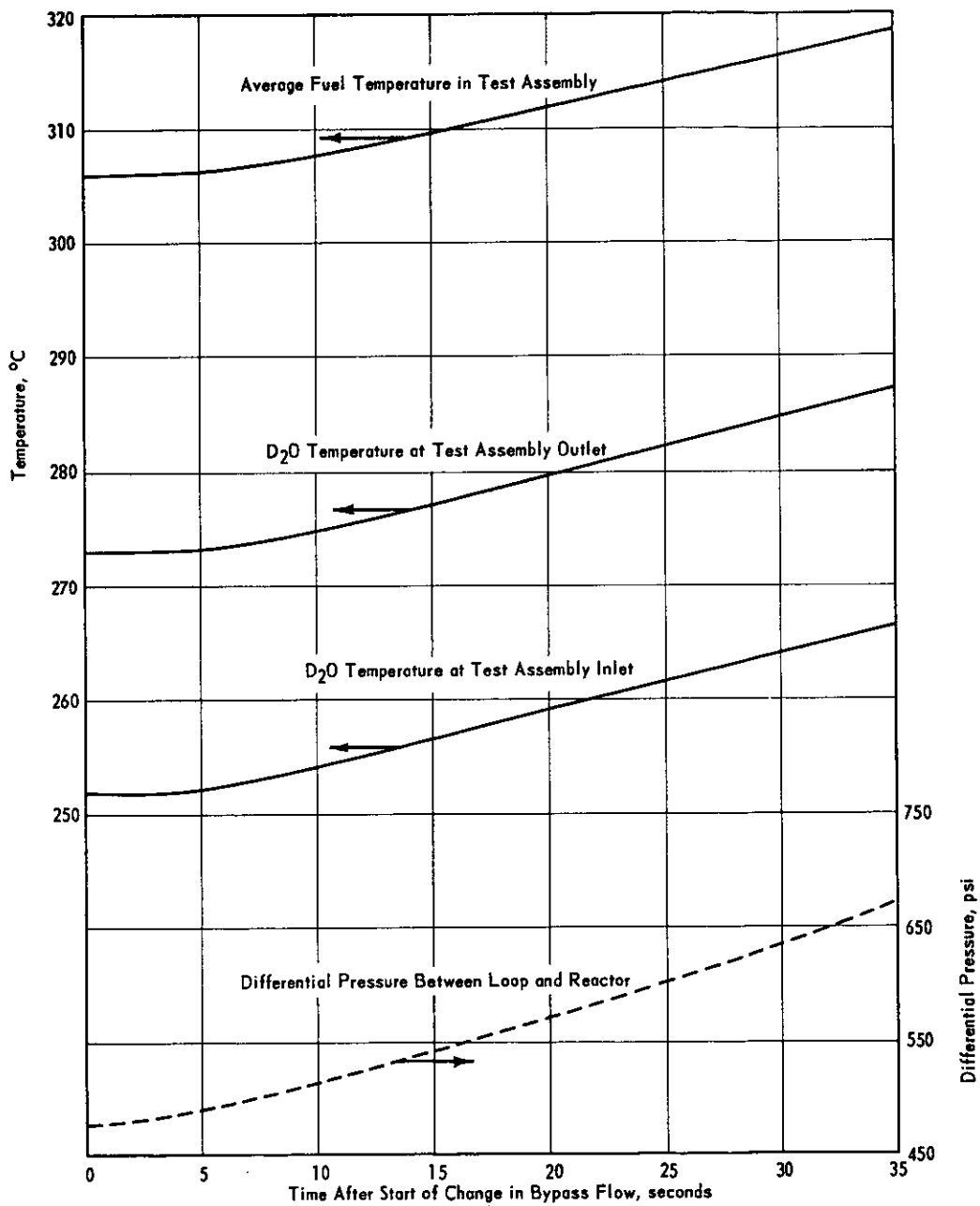


FIG. 6 TRANSIENTS IN LIQUID D<sub>2</sub>O LOOP OF HWCTR AFTER INCREASE IN BYPASS FLOW AROUND LOOP HEAT EXCHANGER

Basis: Bypass flow increases from 90% to 99% of total flow in loop in 5 seconds.

ITEM	REQD	MATERIAL	DESCRIPTION
1	1	Carbon Steel	Flexible Hose
2	1	Carbon Steel	3½" Sch 80 Pipe
3	1	Carbon Steel	5" Sch 160 Pipe Cap
4	1	Carbon Steel	Fuel Bundle Housing
5	1	Carbon Steel	5" ¼ 2½" Sch 80 Reducer
6	2	Carbon Steel	Nozzle
7	1	Carbon Steel	Outer Bayonet Tube
8	1	Carbon Steel	Outer Bayonet Cap
9	1	Carbon Steel	Muff Hold Down Tube
10	1	Carbon Steel	Inner Bayonet Tube
11	1	Carbon Steel	3½" X 2½", Sch 80 Reducer
12	8	Carbon Steel	7/8" Dia X 5½" Lg Stud Bolts / Nuts
13	1	Carbon Steel	3½", 600 lb, Welding Neck Flange
14	1	Carbon Steel	1/8" Thk Asbestos Gasket
15	1	Carbon Steel	3½", 600 lb, Blind Flange
16	2	Carbon Steel	Shock Sleeve
17	1	Carbon Steel	Saddle, 3½"
18	1	Carbon Steel ASTM A-234	Saddle, 5"

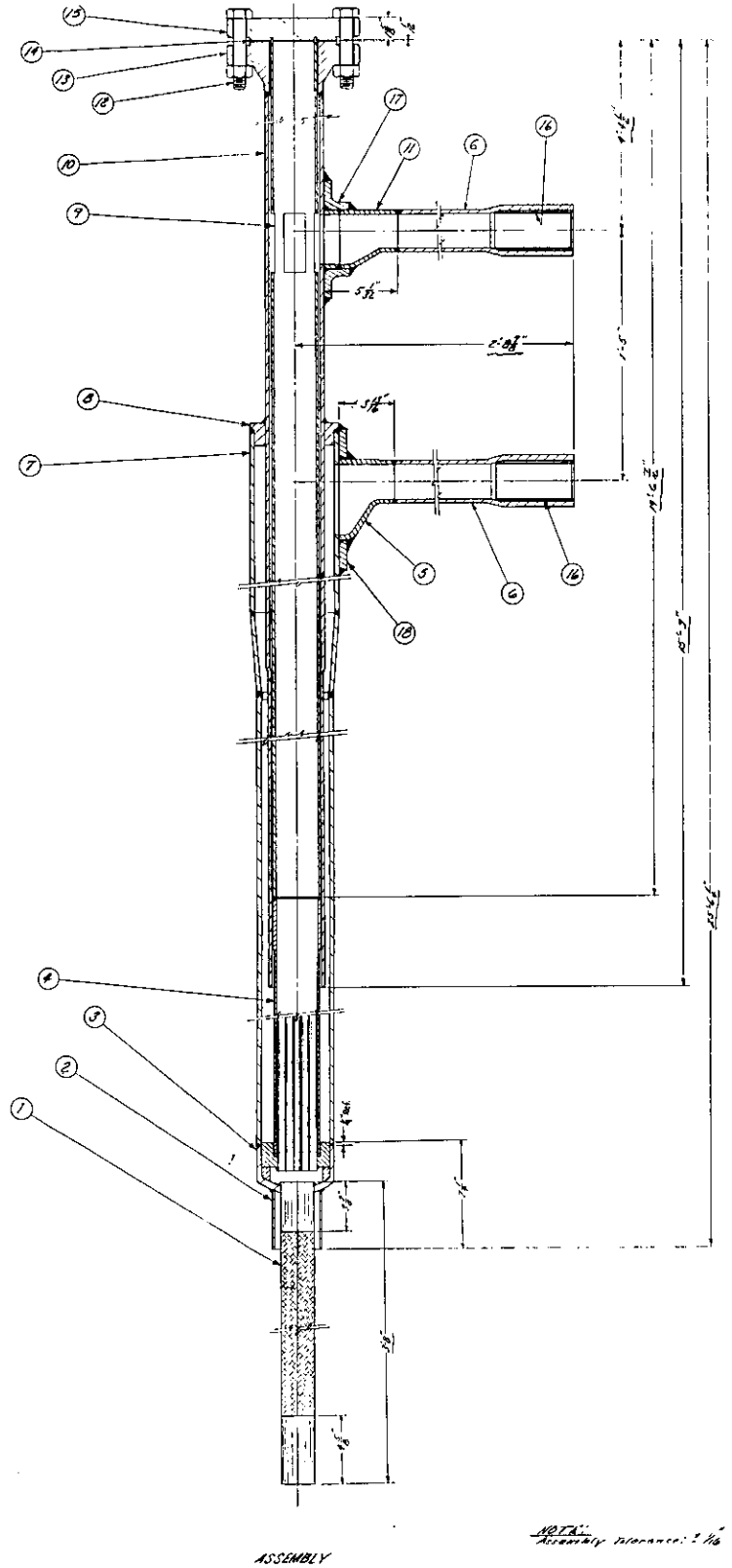


FIG. 7 MOCKUP OF BAYONET FOR HWCTR BOILING D<sub>2</sub>O LOOP

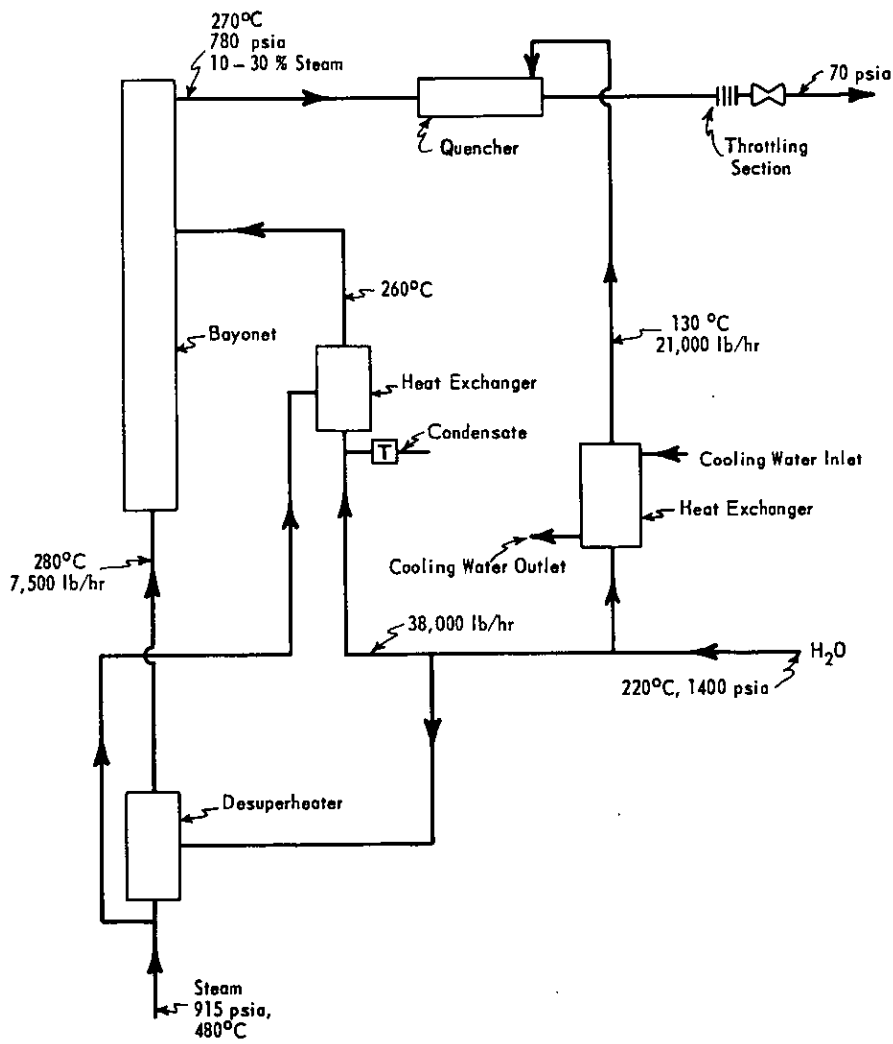


FIG. 8 FLOW DIAGRAM OF HWCTR BAYONET TEST LOOP

ITEM	DESCRIPTION
1	Flexible Steel Hose
2	5-Inch Pipe Cap
3	Pipe Cap Sealing Ring
4	Lower Rod Plate
5	Bayonet Outer Housing Tube
6	Fuel Bundle Housing Tube
7	Fuel Rod (19 Total)
8	Housing Sleeve
9	Housing Ring
10	Rod Adapter
11	Spacing Wire

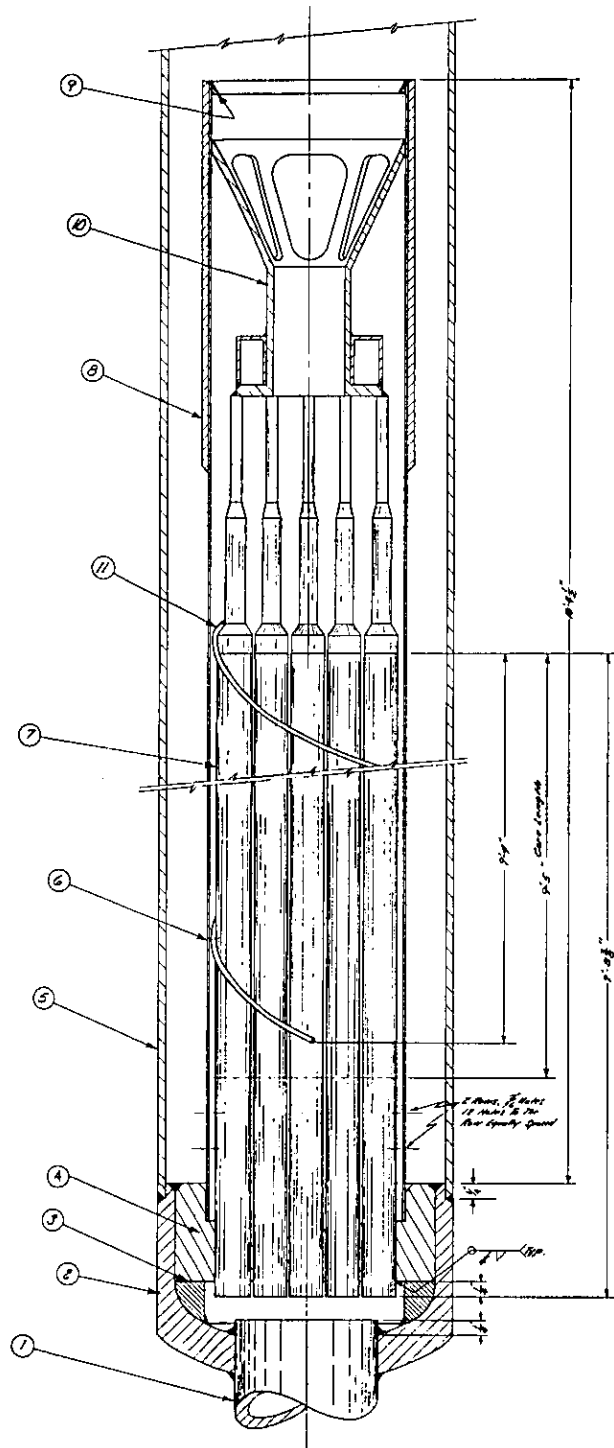


FIG. 9 FUEL ROD BUNDLE FOR MOCKUP OF HWCTR BAYONET



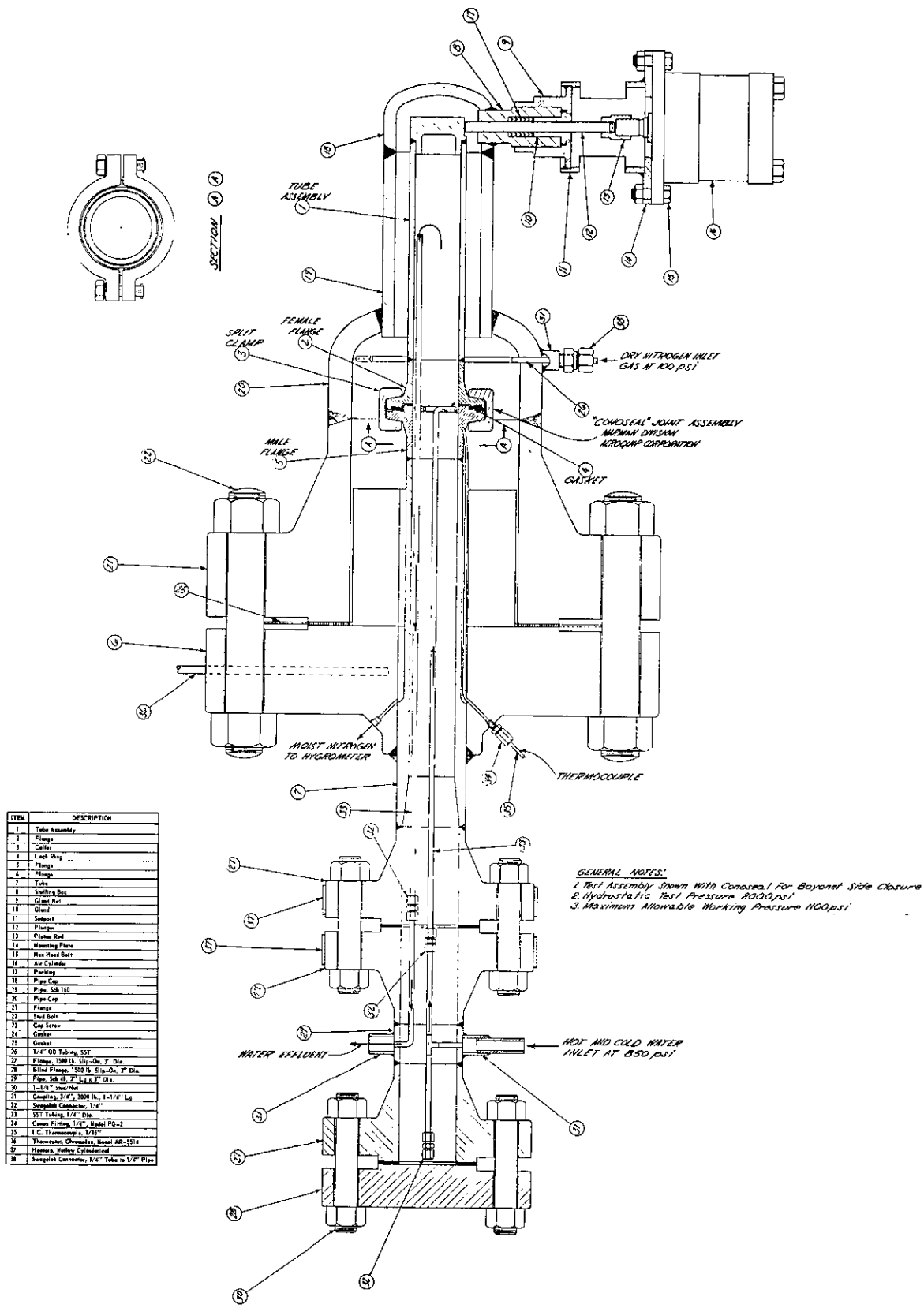


FIG. 11 TEST ARRANGEMENT OF "CONOSEAL" JOINT FOR COOLANT CONNECTIONS OF HWCTR BAYONET

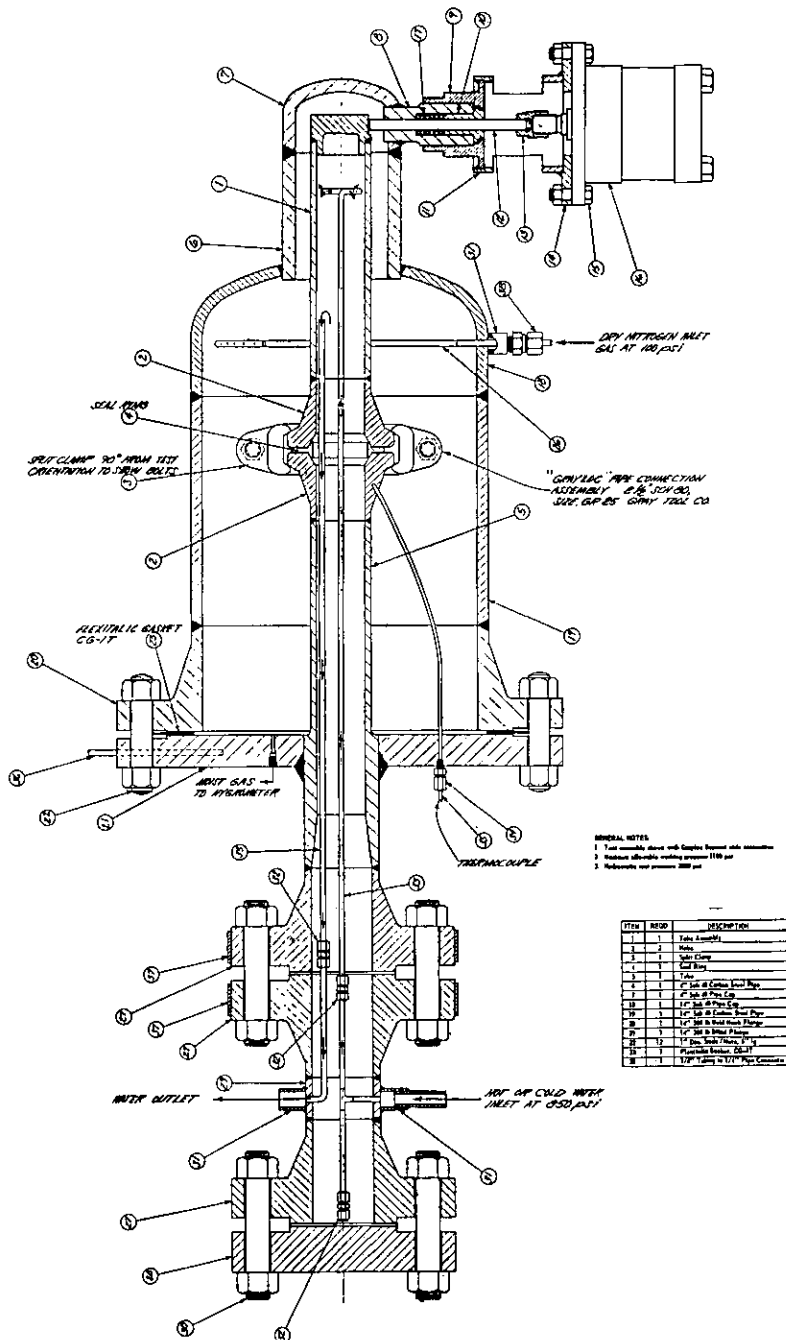
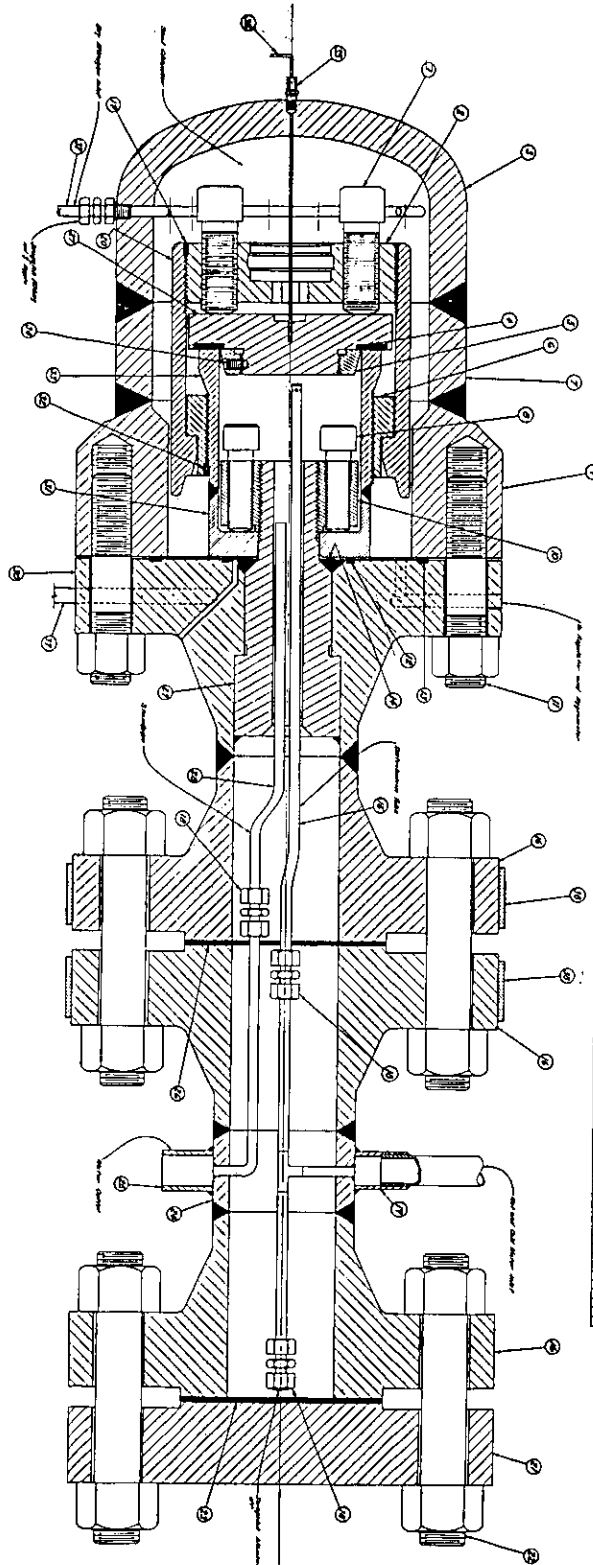


FIG. 12 TEST ARRANGEMENT OF "GRAYLOC" JOINT FOR COOLANT CONNECTIONS OF HWCTR BAYONET

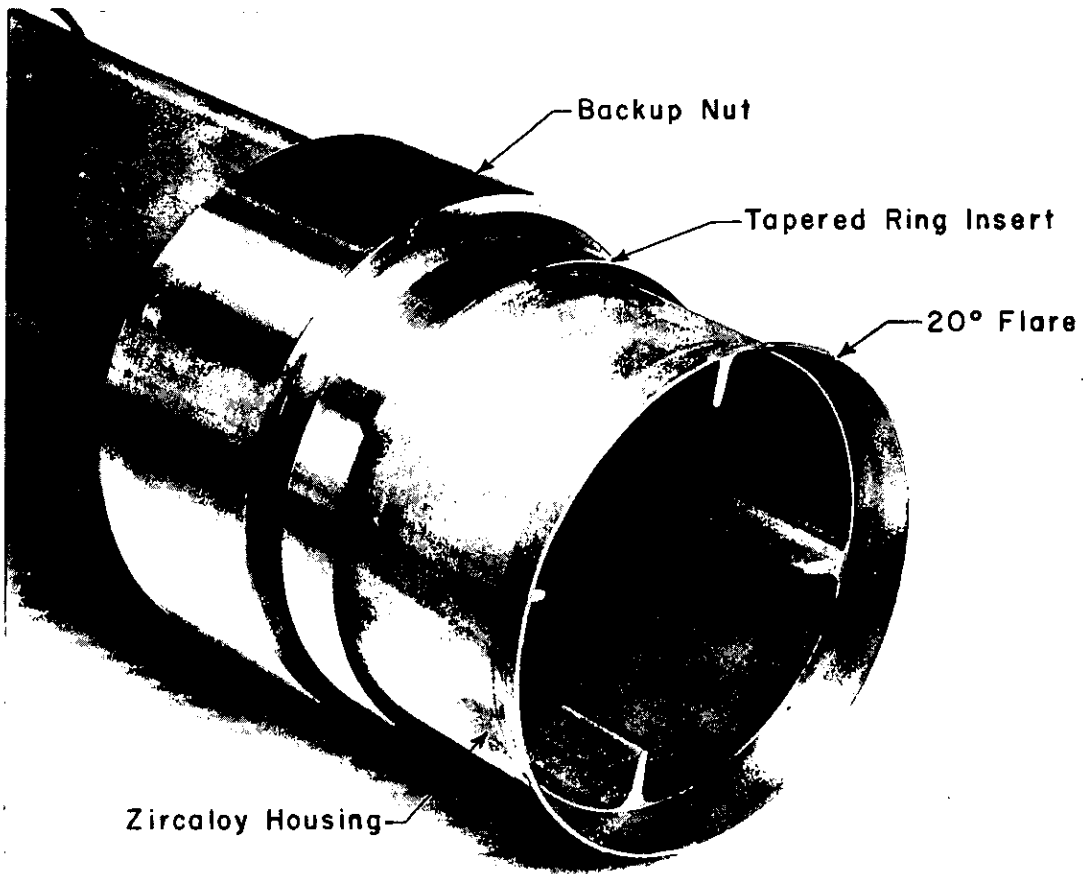


ITEM	DESCRIPTION	REMARKS
1	Cap Screw	
2	Washer	
3	Washer	
4	Washer	
5	Washer	
6	Washer	
7	Washer	
8	Washer	
9	Washer	
10	Washer	
11	Washer	
12	Washer	
13	Washer	
14	Washer	
15	Washer	
16	Washer	
17	Washer	
18	Washer	
19	Washer	
20	Washer	
21	Washer	
22	Washer	
23	Washer	
24	Washer	
25	Washer	
26	Washer	
27	Washer	
28	Washer	
29	Washer	
30	Washer	

**GENERAL NOTES**

1. Test assembly shown with Bayonet Top Closure Type
2. All dimensions to back generator cavity to be indicated and
3. Plating and seal areas shall be indicated and shall be finished to
4. All plating and seal areas shall be indicated and shall be finished to
5. Plating and seal areas shall be indicated and shall be finished to
6. Plating and seal areas shall be indicated and shall be finished to
7. Plating and seal areas shall be indicated and shall be finished to
8. Plating and seal areas shall be indicated and shall be finished to
9. Plating and seal areas shall be indicated and shall be finished to
10. Plating and seal areas shall be indicated and shall be finished to
11. Plating and seal areas shall be indicated and shall be finished to
12. Plating and seal areas shall be indicated and shall be finished to
13. Plating and seal areas shall be indicated and shall be finished to
14. Plating and seal areas shall be indicated and shall be finished to
15. Plating and seal areas shall be indicated and shall be finished to
16. Plating and seal areas shall be indicated and shall be finished to
17. Plating and seal areas shall be indicated and shall be finished to
18. Plating and seal areas shall be indicated and shall be finished to
19. Plating and seal areas shall be indicated and shall be finished to
20. Plating and seal areas shall be indicated and shall be finished to
21. Plating and seal areas shall be indicated and shall be finished to
22. Plating and seal areas shall be indicated and shall be finished to
23. Plating and seal areas shall be indicated and shall be finished to
24. Plating and seal areas shall be indicated and shall be finished to
25. Plating and seal areas shall be indicated and shall be finished to
26. Plating and seal areas shall be indicated and shall be finished to
27. Plating and seal areas shall be indicated and shall be finished to
28. Plating and seal areas shall be indicated and shall be finished to
29. Plating and seal areas shall be indicated and shall be finished to
30. Plating and seal areas shall be indicated and shall be finished to

FIG. 13 TEST ARRANGEMENT OF TOP CLOSURE FOR HWCTR BAYONET



Mag. 1X

FIG. 14 ZIRCALOY HOUSING FLARED JOINT

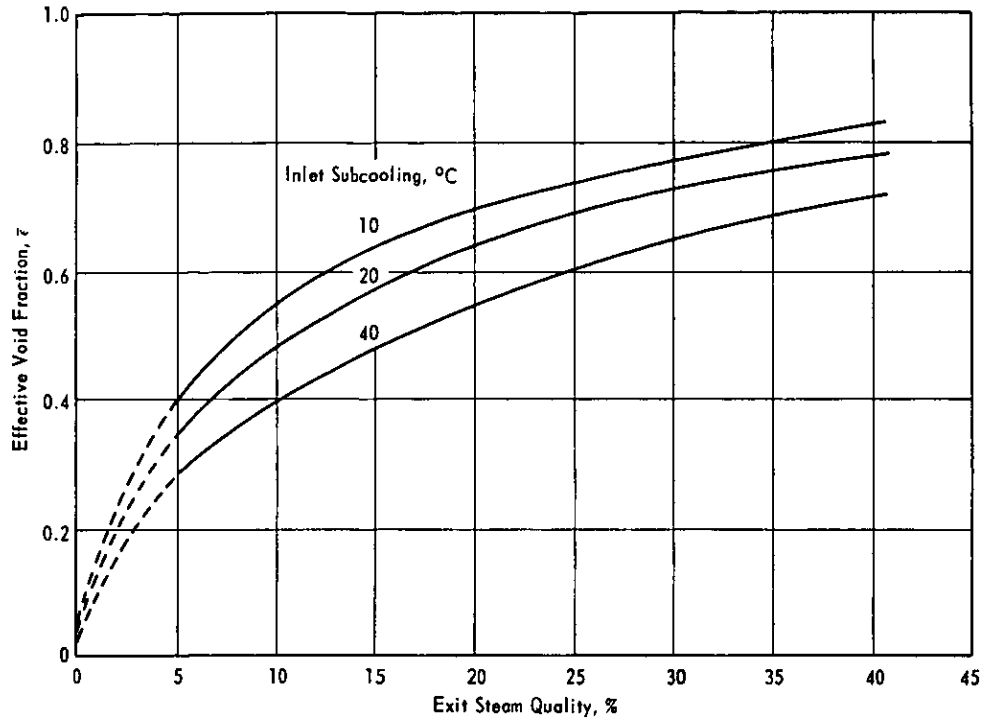


FIG. 15 EFFECTIVE VOID FRACTION IN A BOILING D<sub>2</sub>O REACTOR

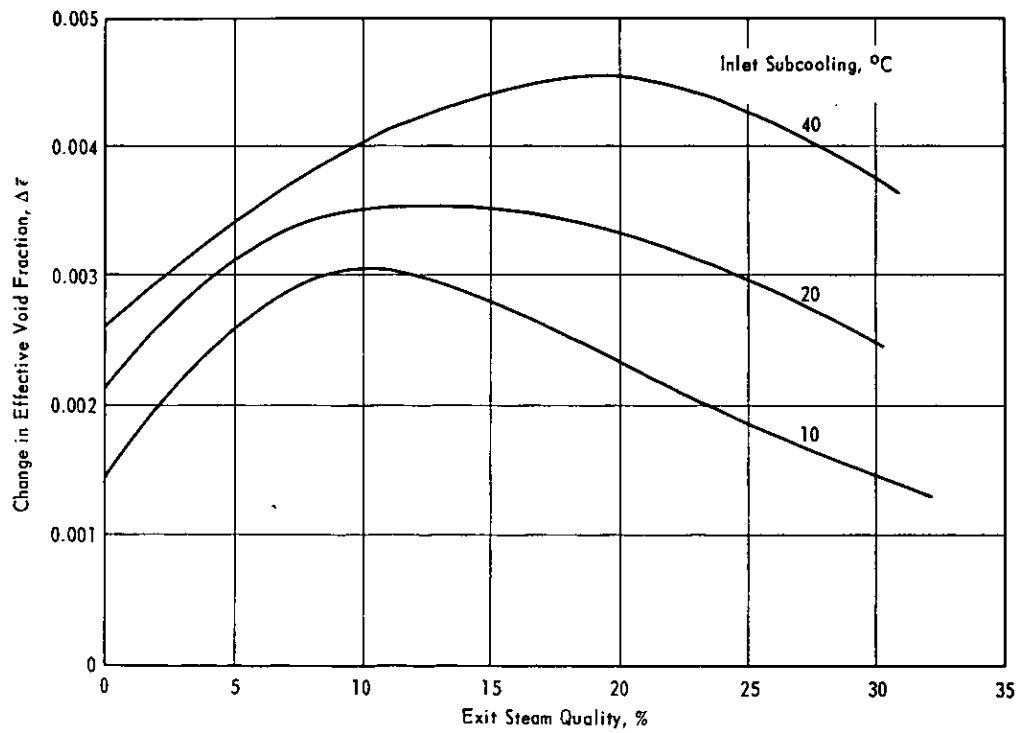


FIG. 16 EFFECT OF A 1% INCREASE IN POWER ON THE VOID FRACTION IN A BOILING D<sub>2</sub>O REACTOR

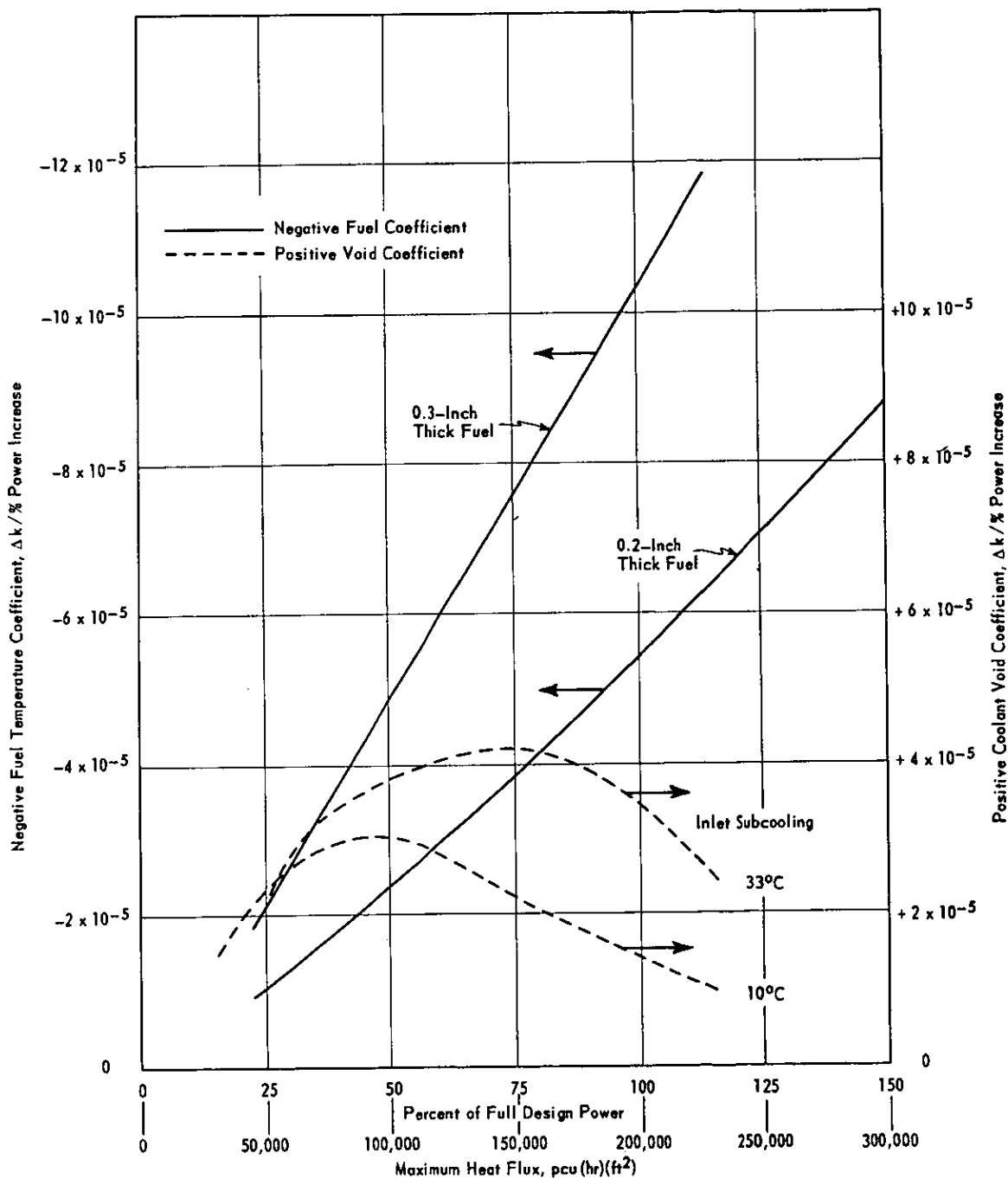


FIG. 17 POWER COEFFICIENTS OF REACTIVITY FOR BOILING-D<sub>2</sub>O-COOLED POWER REACTORS FUELED WITH UO<sub>2</sub> TUBES

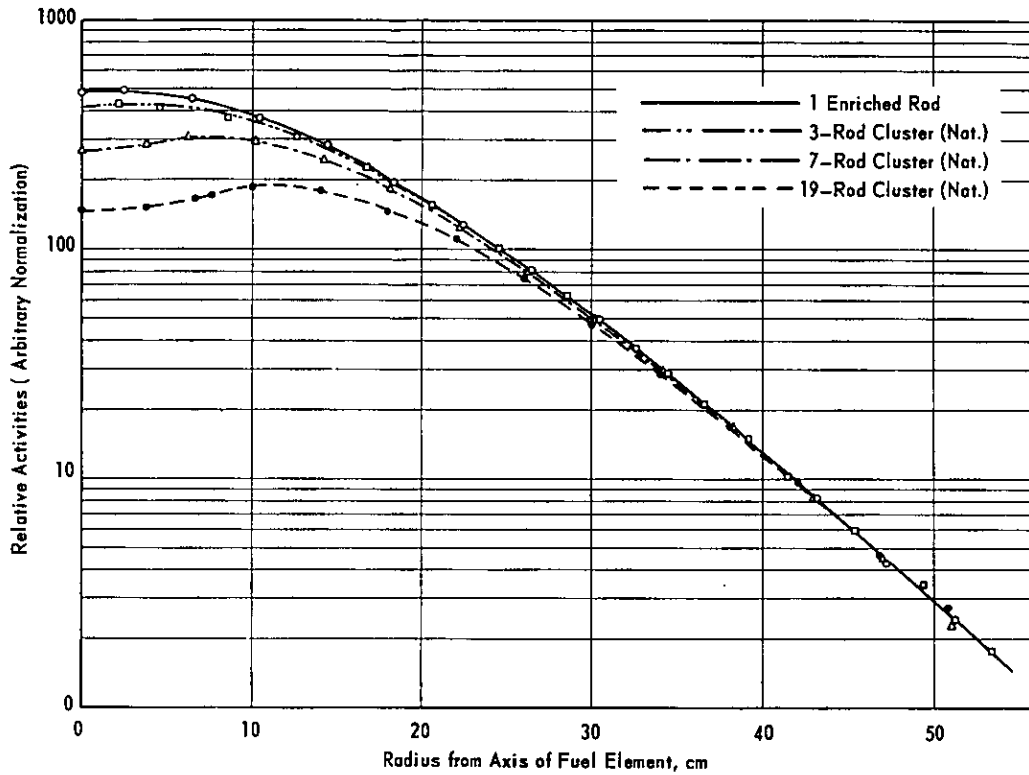


FIG. 18 INDIUM FOIL ACTIVITY DISTRIBUTIONS FROM VARIOUS SOURCES

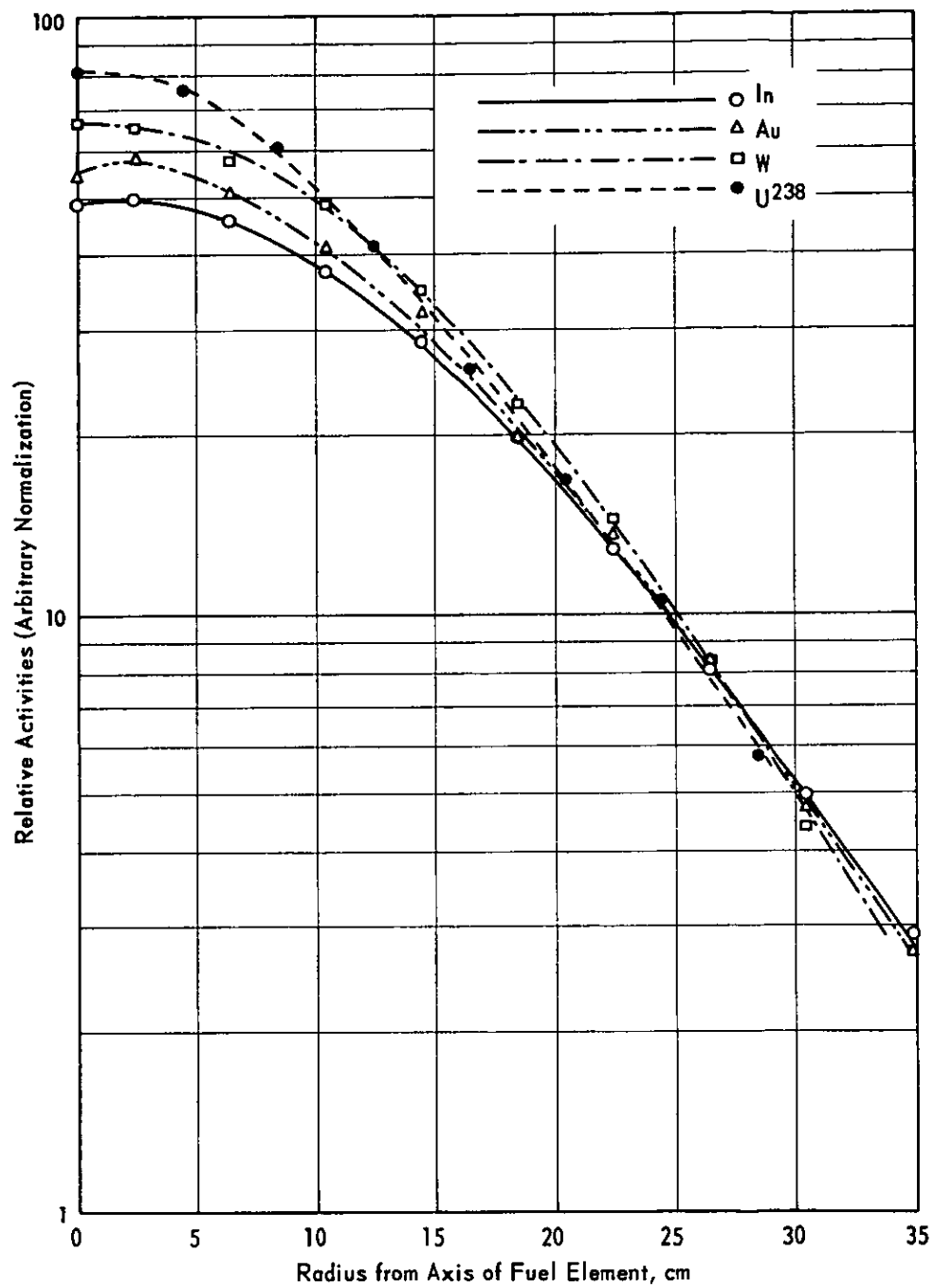


FIG. 19 FOIL ACTIVITY DISTRIBUTIONS WITH A SINGLE ENRICHED URANIUM ROD AS A SOURCE

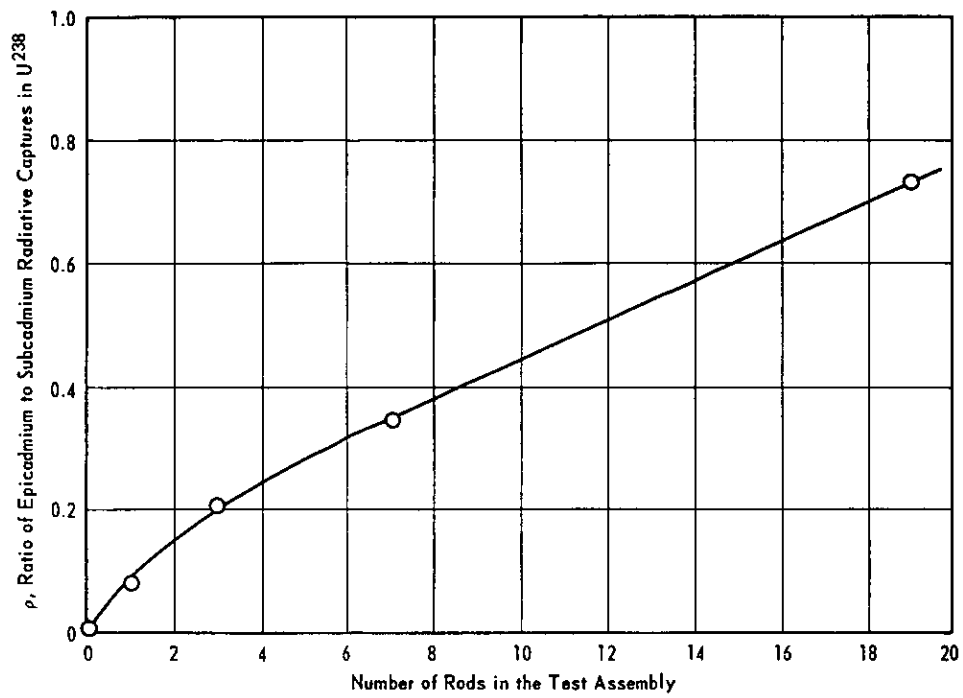
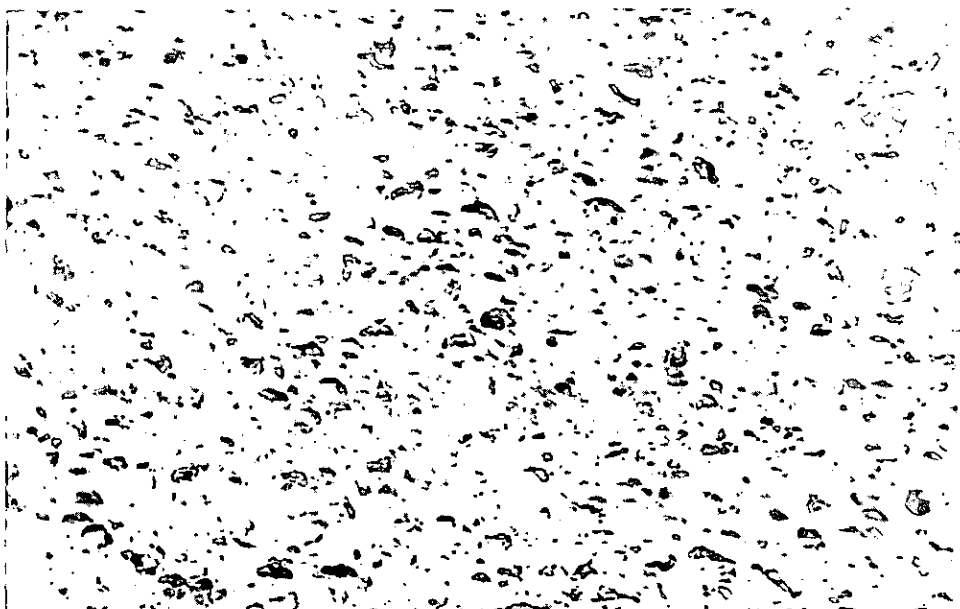


FIG. 20 SELF-RESONANCE CAPTURE RATIO FOR ISOLATED FUEL ELEMENTS IN D<sub>2</sub>O



Neg. 28351 a. Section Showing a Large Amount of Alpha Uranium Mag. 500X

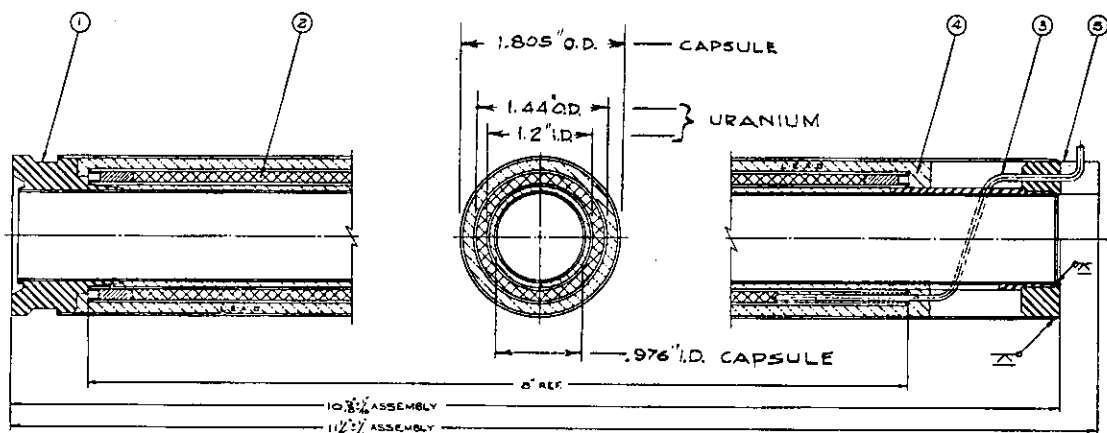
White phase was identified as alpha uranium by X-ray diffraction studies of the area shown.



Neg. 28365 b. Section Showing the Typical Amount of Alpha Uranium Mag. 500X

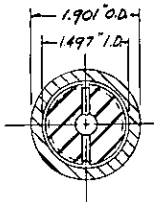
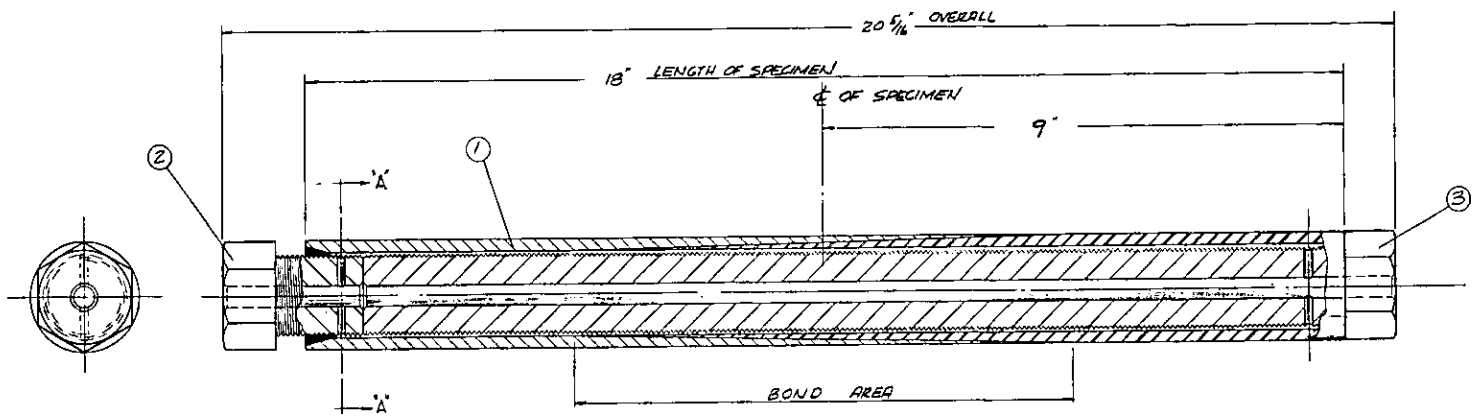
Trace amounts of the white phase, shown above, did not give a diffraction pattern.

FIG. 21 URANIUM METAL IMPURITY IN FUSED  $UO_2$



ITEM	DESCRIPTION
1	Insulated Uranium Can Sub-Assembly
2	Coextruded Zircaloy Clad Fuel Tube Assembly
3	Thermocouple
4	Lead
5	Thermocouple Top Plug
6	Top Plug

FIG. 22 LEAD-INSULATED TUBULAR URANIUM SPECIMEN

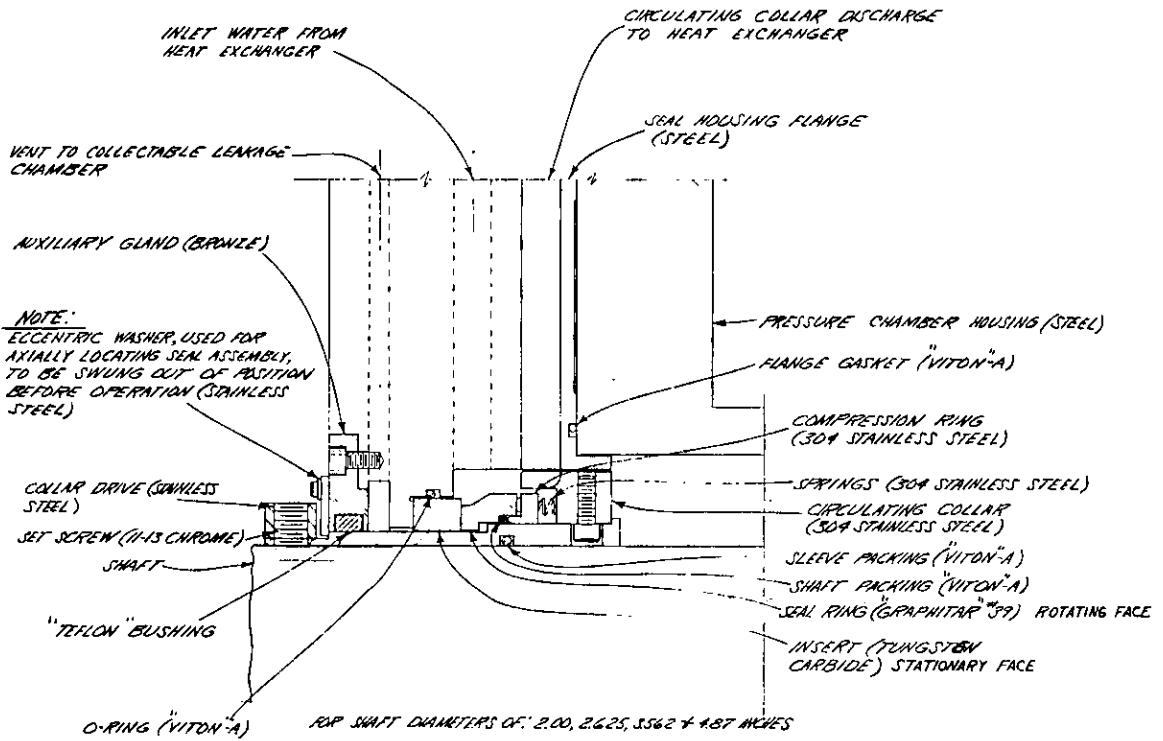


ZIRCALOY - STAINLESS JOINT IRRADIATION SPECIMEN

ITEM	REQD	DESCRIPTION
1	1	Specimen
2	1	Short Bolt
3	1	Long Bolt

SECTION "A-A"

FIG. 23 IRRADIATION SPECIMEN OF A TANDEM-EXTRUDED JOINT OF ZIRCALOY TO STAINLESS STEEL



DESIGN CONDITIONS:  
 TEMP - 280°C  
 PRESSURE - 100 TO 1000 PSIG  
 RPM - 500 TO 3500

"DURAMETALLIC" CORPORATION SEAL ASSEMBLY

FIG. 24 "DURAMETALLIC" MECHANICAL SEAL FOR BENCH TESTING

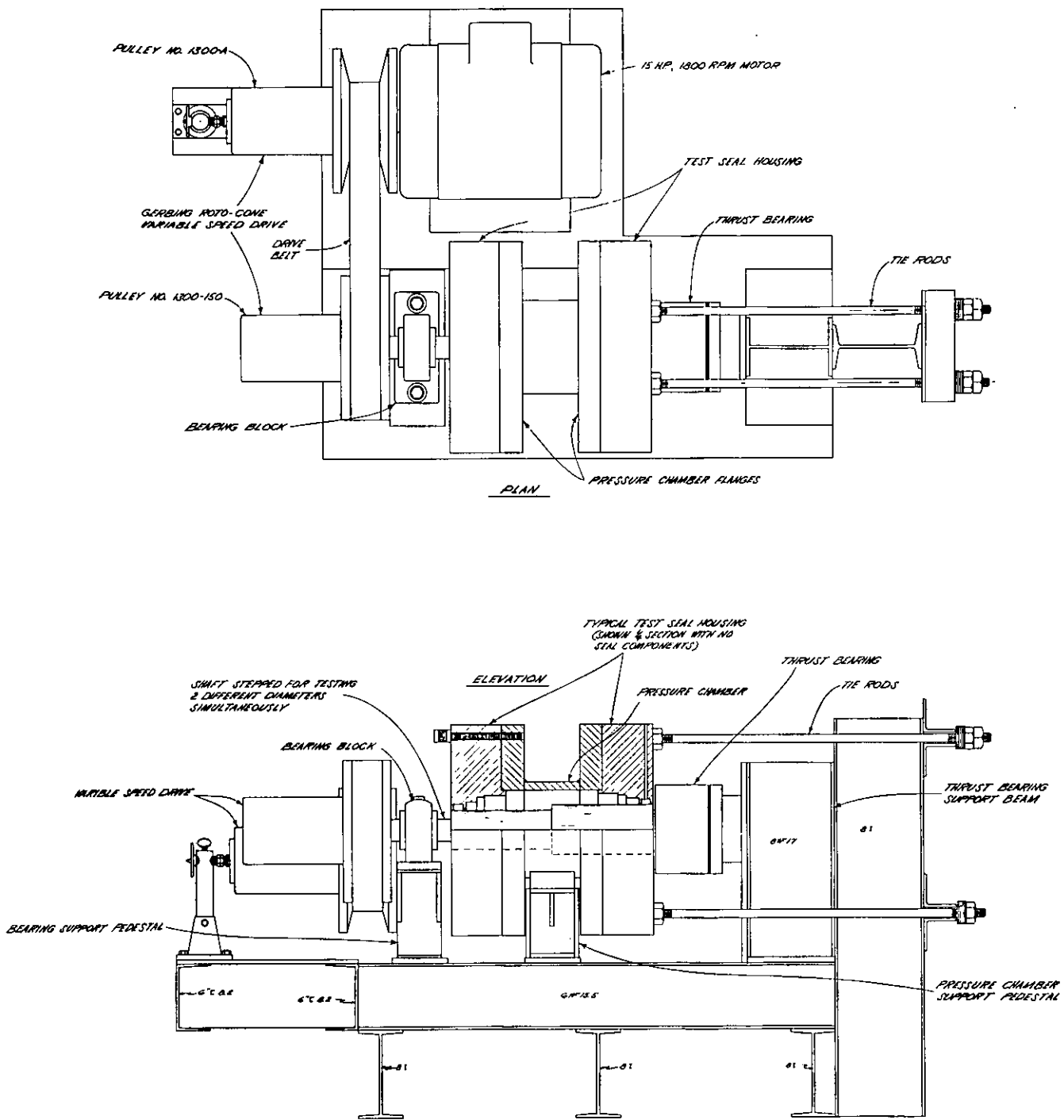


FIG. 25 BENCH TESTER FOR MECHANICAL SEALS